Simulation studies of molecule and ion transport in hydrogen bonded media

Materials Simulations in Earth and Planetary Sciences Seminar Series, Columbia University

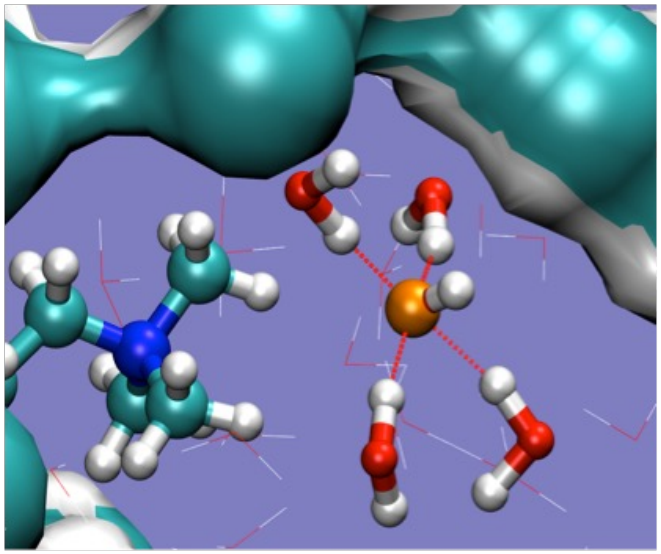

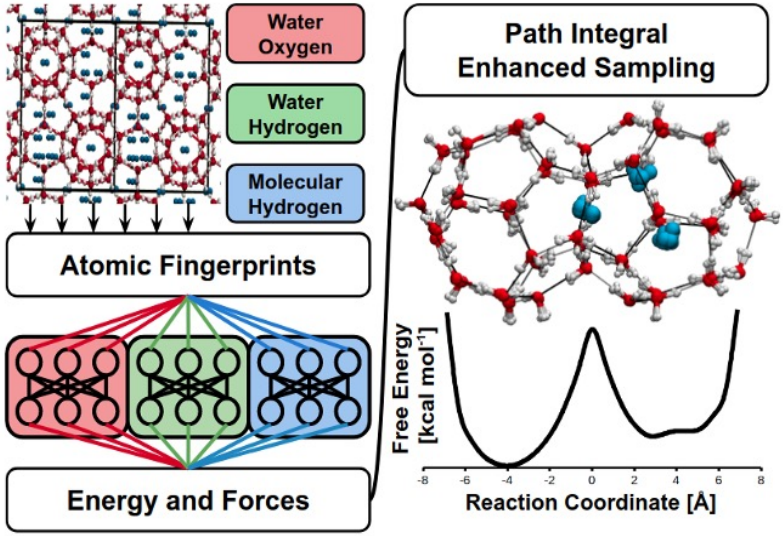

Mark E. Tuckerman

Chair of Chemistry, Professor of Chemistry and Mathematics

Dept. of Chemistry and Courant Institute of Mathematical Sciences

New York University, 100 Washington Square East, NY 10003

NYU-ECNU Center for Computational Chemistry at NYU Shanghai 200062, China

华 东 师 范 大 学-纽约大学 计算化学联合研究中心

Climate change: Coming into focus after COVID?

Li ion battery:

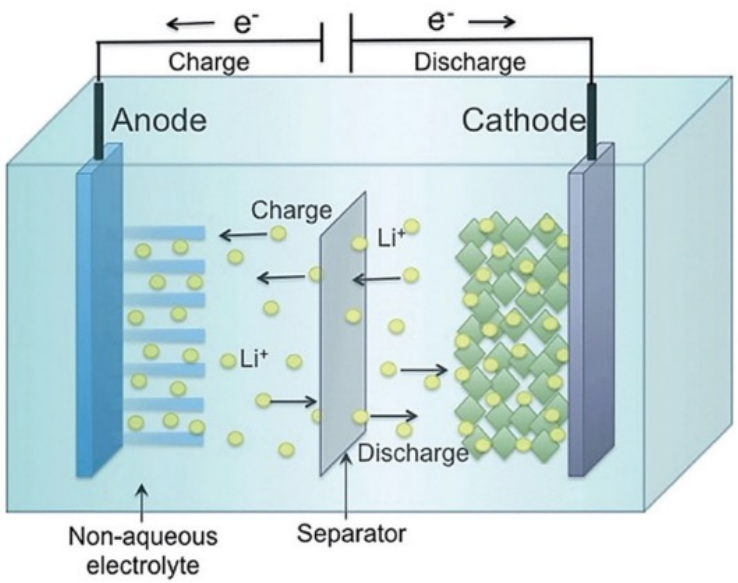

PEM fuel cell:

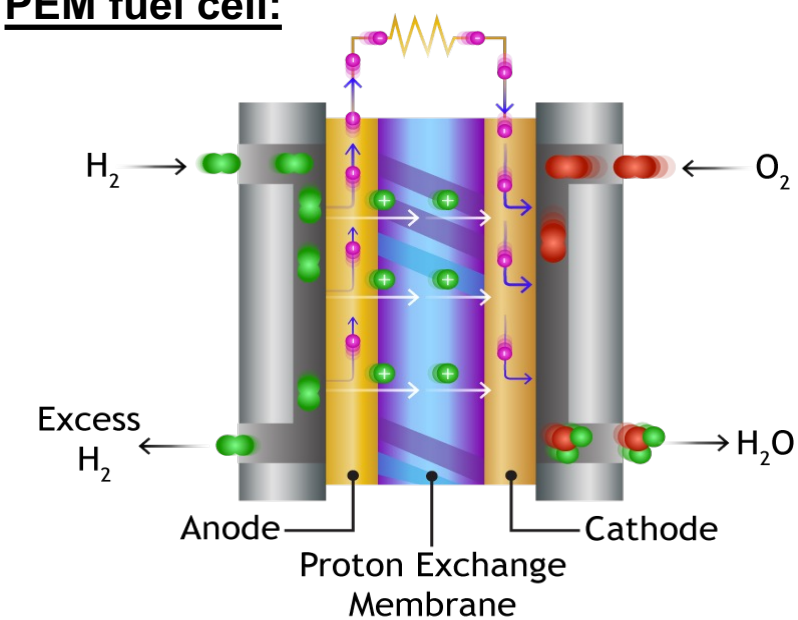

Fuel cells versus batteries

Why Fuel cells?

- Ease of filling versus recharging.
- No harmful emissions.
- No need for mining of crucial metals (lithium, nickel, cobalt,…).
- CO_2 production in H_2 production versus metal recycling.
- Higher energy density by weight, allowing greater range.

Challenges

- Still not cost-effective.
- Durability issues.
- On-board hydrogen storage challenges.
- Fuel cells only versus fuel-cell enhancement of battery performance?

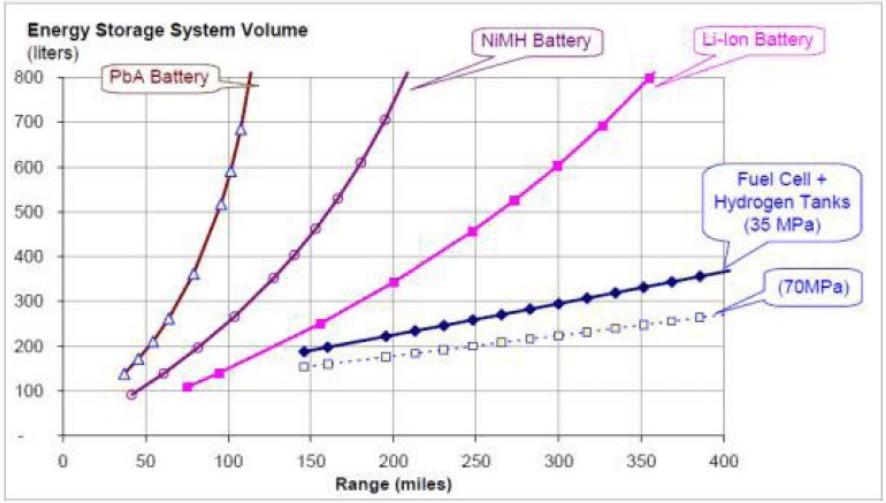

PbA = lead acid; NiMH = nickel metal hydride; Li-Ion = lithium ion; MPa = megapascal, a unit of pressure (1MPa = 145 psi). Source: Cadex Electronics (CH)

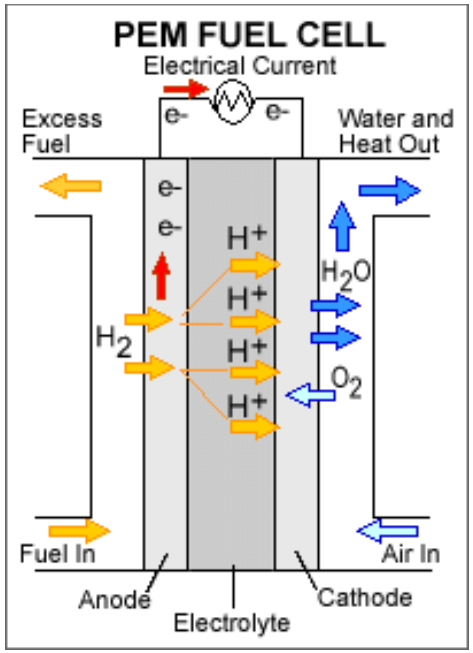

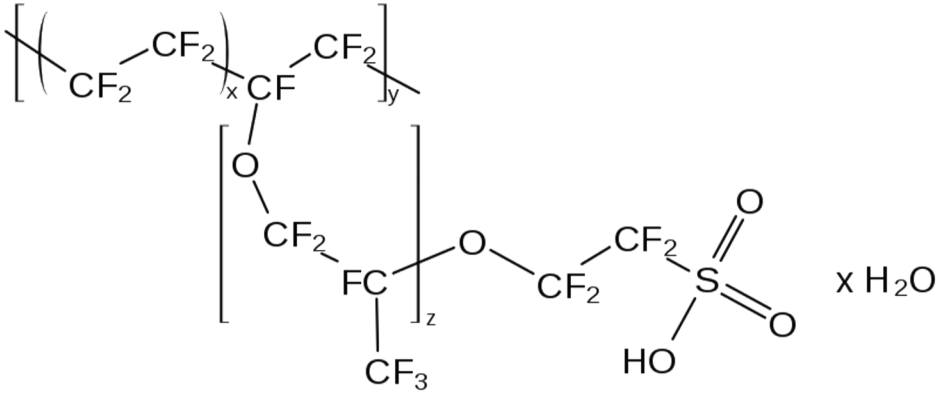

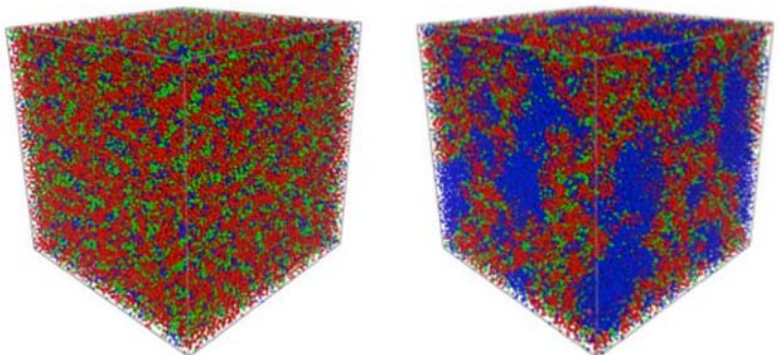

D. Wu, S. J. Paddison, J. A. Elliott, S. J. Hamrock *Langmuir* **26** (2010).

Anode: $2H_2 \rightarrow 4H^+ + 4e^-$

Cathode: $O_2 + 4e^- + 4H^+ \rightarrow 2H_2O$

Overall: $2H_2 + O_2 \rightarrow 2H_2O$

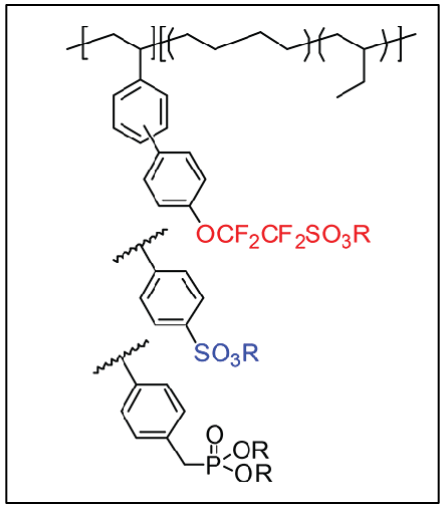

Bae and coworkers *Macromolec.* (2018).

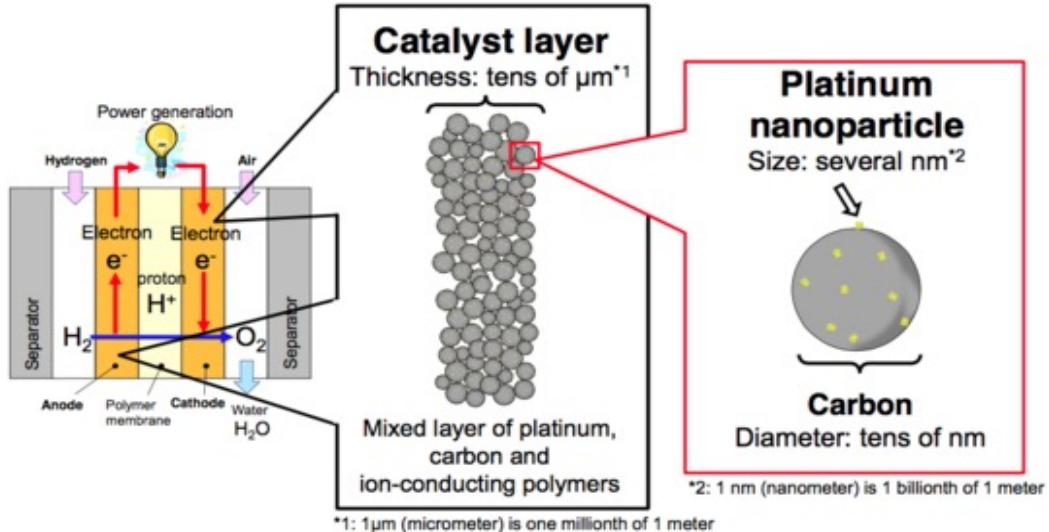

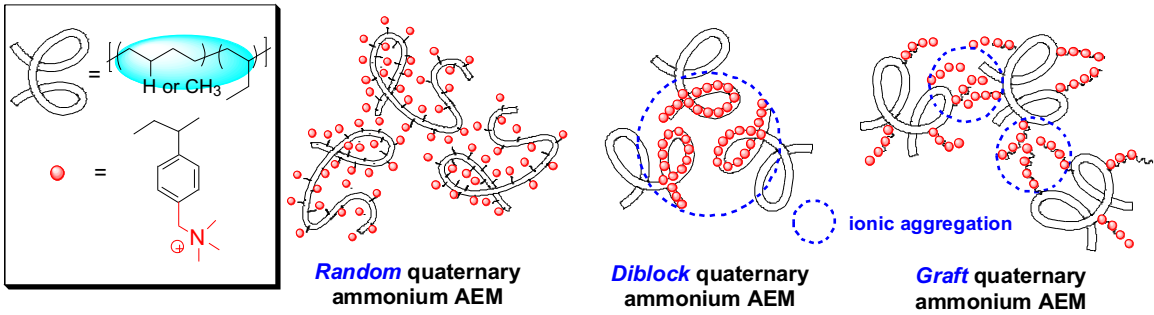

Triblock copolymer:

Polystyrene-b-poly(ethylene-co-butylene)-b-polystyrene (SEBS)

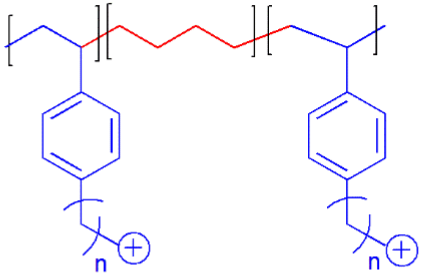

SEBS AEMs
(n = 1, 3, 5)

Anode: $2H_2 + 4OH^- \rightarrow 4H_2O + 4e^-$

Cathode: $O_2 + 2H_2O + 4e^- \rightarrow 4OH^-$

Overall: $2H_2 + O_2 \rightarrow 2H_2O$

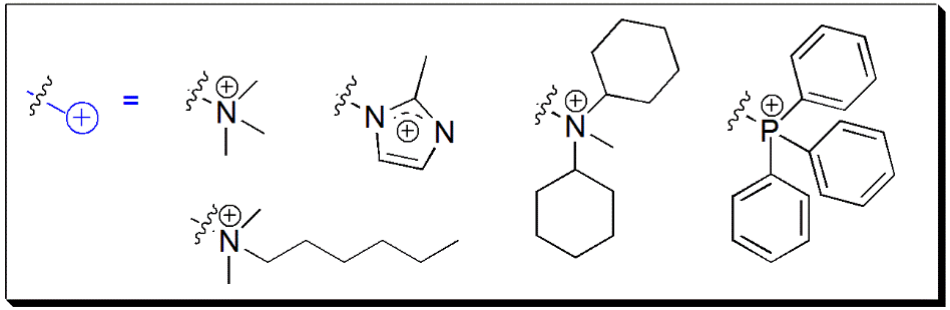

Advantages of AEMs

1. No precious metal catalysts
2. Reverse electro-osmotic flow means better water management
3. Much less known about AEMs compared to PEMs. Design principles needed.

AEM fuel cells among the first to be developed.

Used to power on-board systems in Apollo missions

From morphologies to idealized geometries

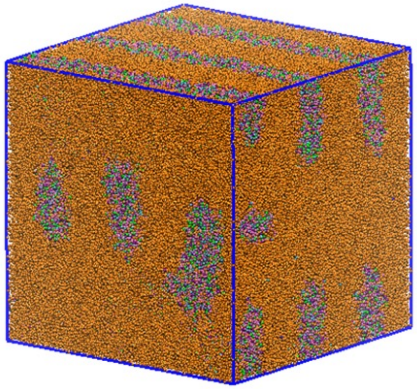

$\lambda = \frac{n_{\mathrm{H2O}}}{n_{\mathrm{cation}}}$

$\lambda = 4$

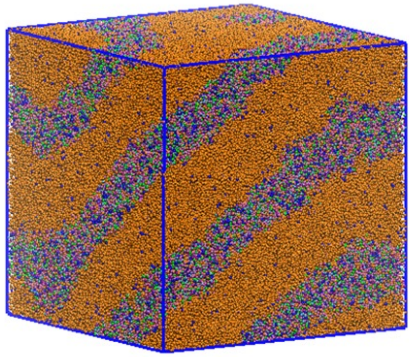

$\lambda = 8$

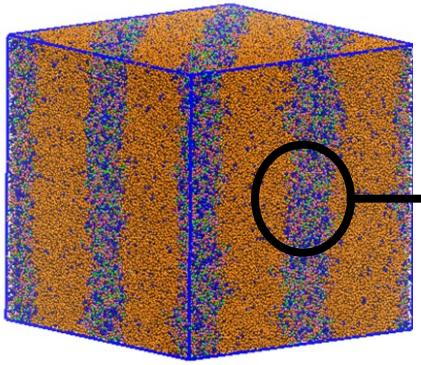

$\lambda = 12$

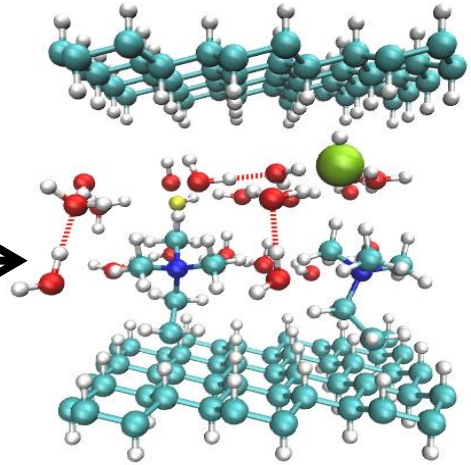

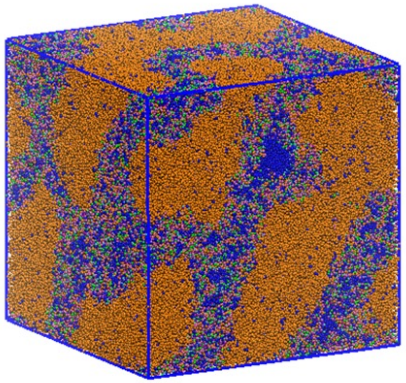

$\lambda = 16$

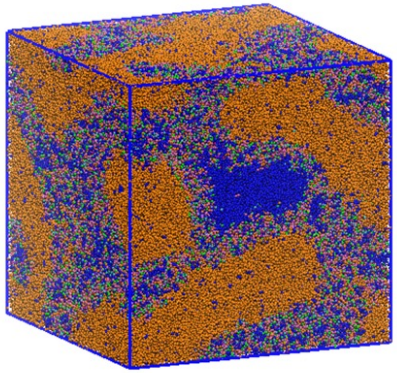

$\lambda = 20$

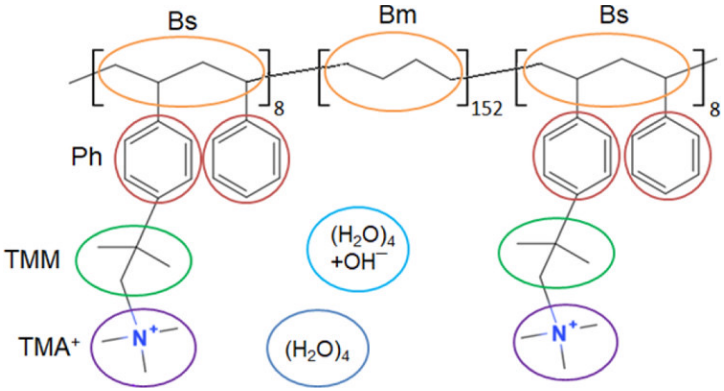

Dissipative particle dynamics (DPD) simulations:
F. Sepehr, H. Liu, C. Bae, MET, M. A. Hickner, S. J. Paddison
Macromolec.. **50**, 4397 (2017).

- Qualitative change in morphology with hydration
- Exclusive water domains at $\lambda = 16$ and 20

$$M_i \ddot{\mathbf{R}}_i = \sum_{j \neq i} \left[\mathbf{F}_{ij}^C + \mathbf{F}_{ij}^D + \mathbf{F}_{ij}^R \right] + \mathbf{f}_i^{\mathrm{bonded}}$$

1806:

Theodor v. Grotthuss

MÉMOIRE

Sur la décomposition de l'eau et des corps qu'elle tient en dissolution à l'aide de l'électricité galvanique,

PAR C. J. T. DE GROTTHUSS (1).

CHAPITRE PREMIER.

Action de l'électricité galvanique sur certains corps dissous dans l'eau.

§. PREMIER.

SANS m'arrêter à la discussion d'une foule d'hypothèses imaginées pour expliquer la décomposition de l'eau par l'appareil électromoteur, j'exposerai une théorie générale de la décomposition des liquides par l'électricité galvanique, qui me paroît réduire les effets de celle-ci à une explication simple

(1) Ce Mémoire a été imprimé à Rome en 1805. Nous avons pensé qu'on le trouveroit ici avec plaisir, et l'auteur lui-même à desiré qu'on le réimprimât.

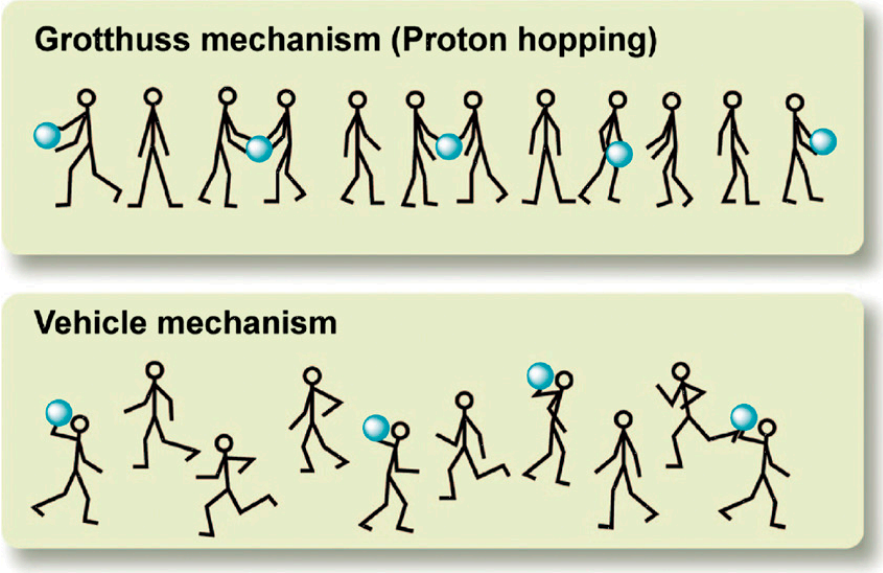

Ab initio molecular dynamics (AIMD)

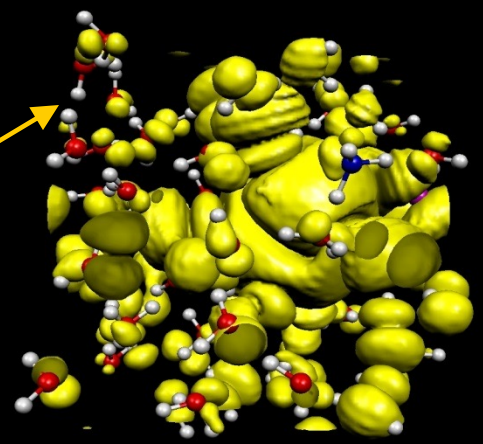

Electrons

Kohn-Sham DFT [BLYP + DCACP + PW]

$$\left[-\frac{\nabla^2}{2}+V_{\mathrm{KS}}[n](\mathbf{r},\mathbf{R})\right]\psi_i(\mathbf{r})=\varepsilon_i\psi_i(\mathbf{r})$$

Nuclei

Newton's 2nd law:

$$\mathbf{F}_I = M_I \frac{d^2\mathbf{R}_I}{dt^2}$$

Start with nuclei → Add electrons → Compute → $n_0(\mathbf{r}),\{\psi_i(\mathbf{r})\} \Rightarrow \mathbf{F}_I$

↓

Move nuclei with $\mathbf{F}_I$ → Add electrons

$$\mathbf{R}_I(t+\Delta t)=\mathbf{R}_I(t)+\Delta t\dot{\mathbf{R}}_I(t)+\frac{\Delta t^2}{2M_I}\mathbf{F}_I(t)$$

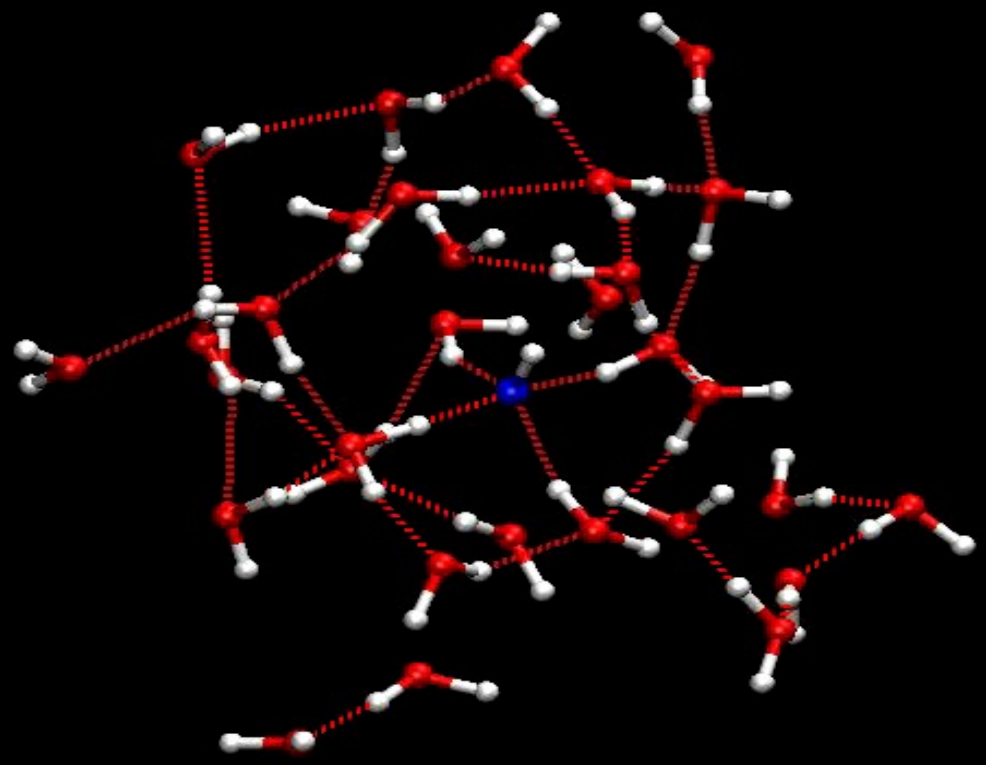

From Z. Ma and MET *Chem. Phys. Lett*. **511**, 177 (2011)
32 water molecules + 1 OH- in 10 Å periodic box run for 80 ps
Exchange-correlation = BLYP + DCACP, Code = PINY_MD
Basis set = Discrete Variable Representation [H. S. Lee and MET *JPCA* (2006)]

Bulk aqueous transport mechanism [MET *et al. ACR* (2006)]

Lewis Structure:

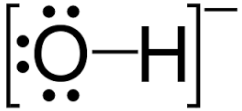

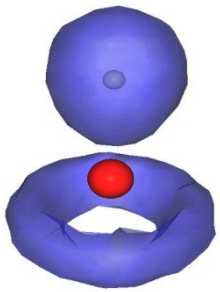

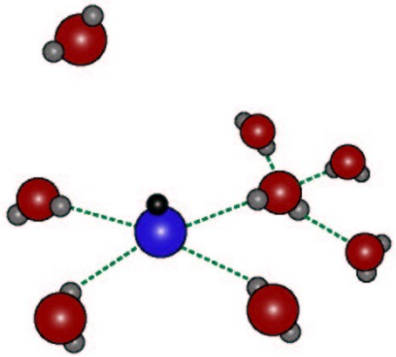

4-coordinate "resting" state

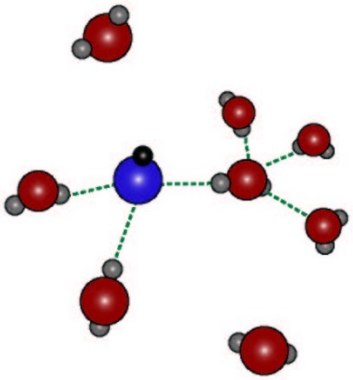

3-coordinate "active" state

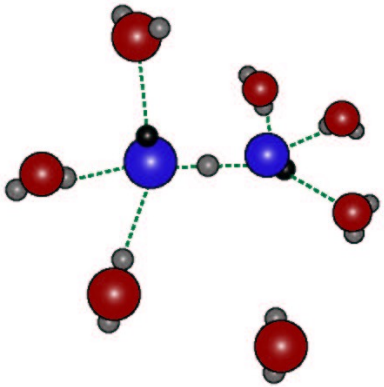

Donated H-bond "presolvates" leading to PT

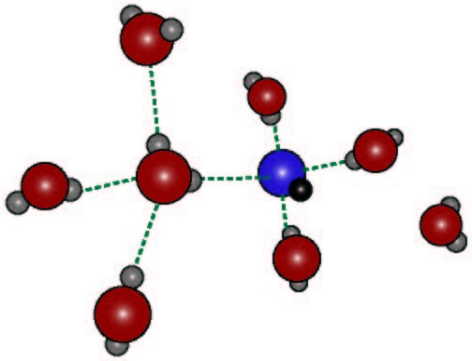

New 4-coordinate state closes gate

$$\frac{D_{OH^-}}{D_{H_3O^+}} = \frac{0.45}{0.80} = 0.56 \quad \text{Expt.: } 0.47$$

Comparing IR spectra and diffusion

From Roberts, *et al*. PNAS **106** (2009)

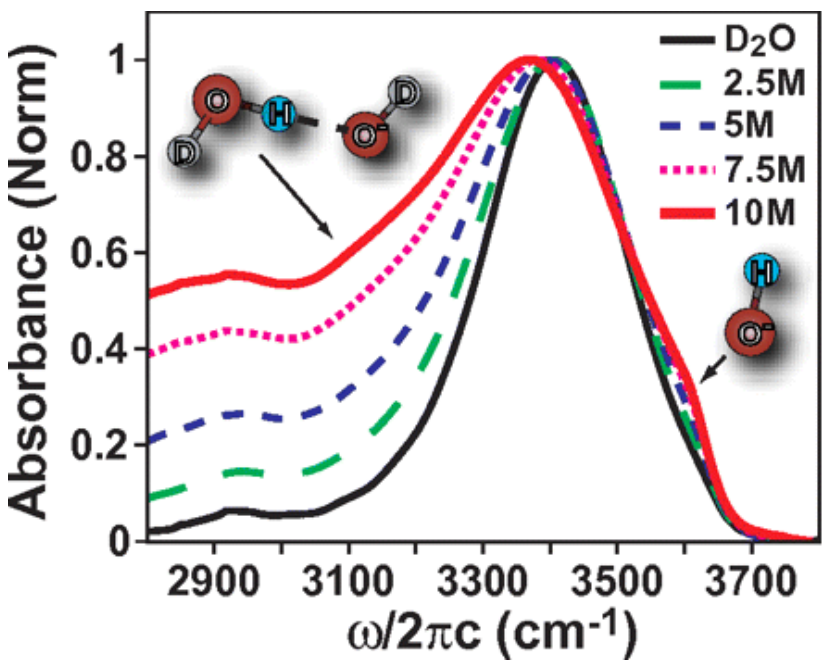

14 M KOH IR spectrum
Expt.: Librovich and Maiorov,
Russian J. Phys. Chem. **56**, 624 (1982)

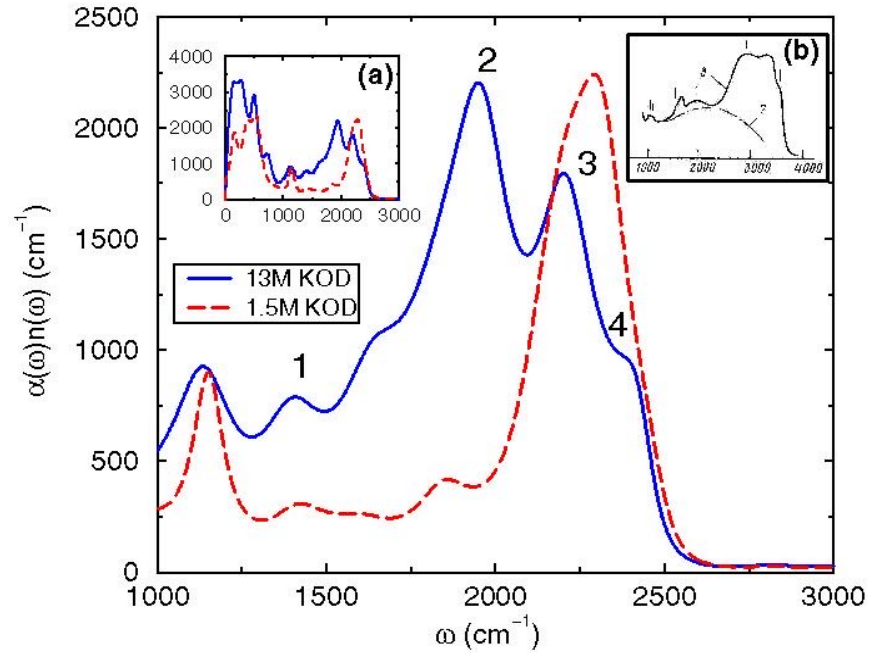

Z. W. Zhu and MET *J. Phys. Chem. B* **106**, 8009 (2002).

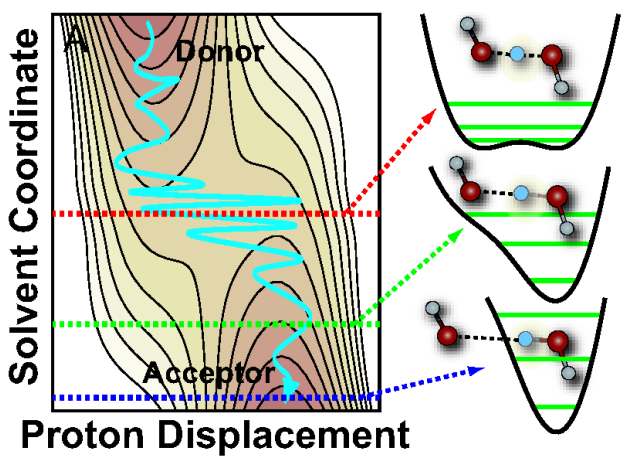

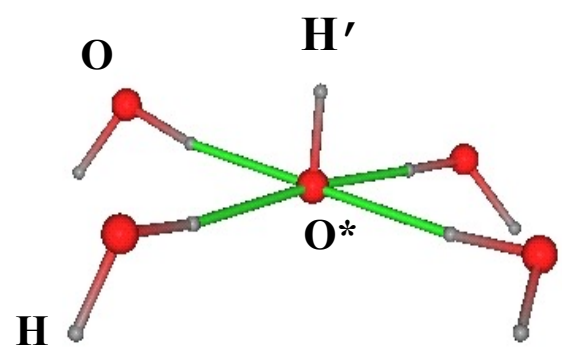

Example structures studied

$$\rho = \frac{m_W}{V_B - V_{cat}}$$

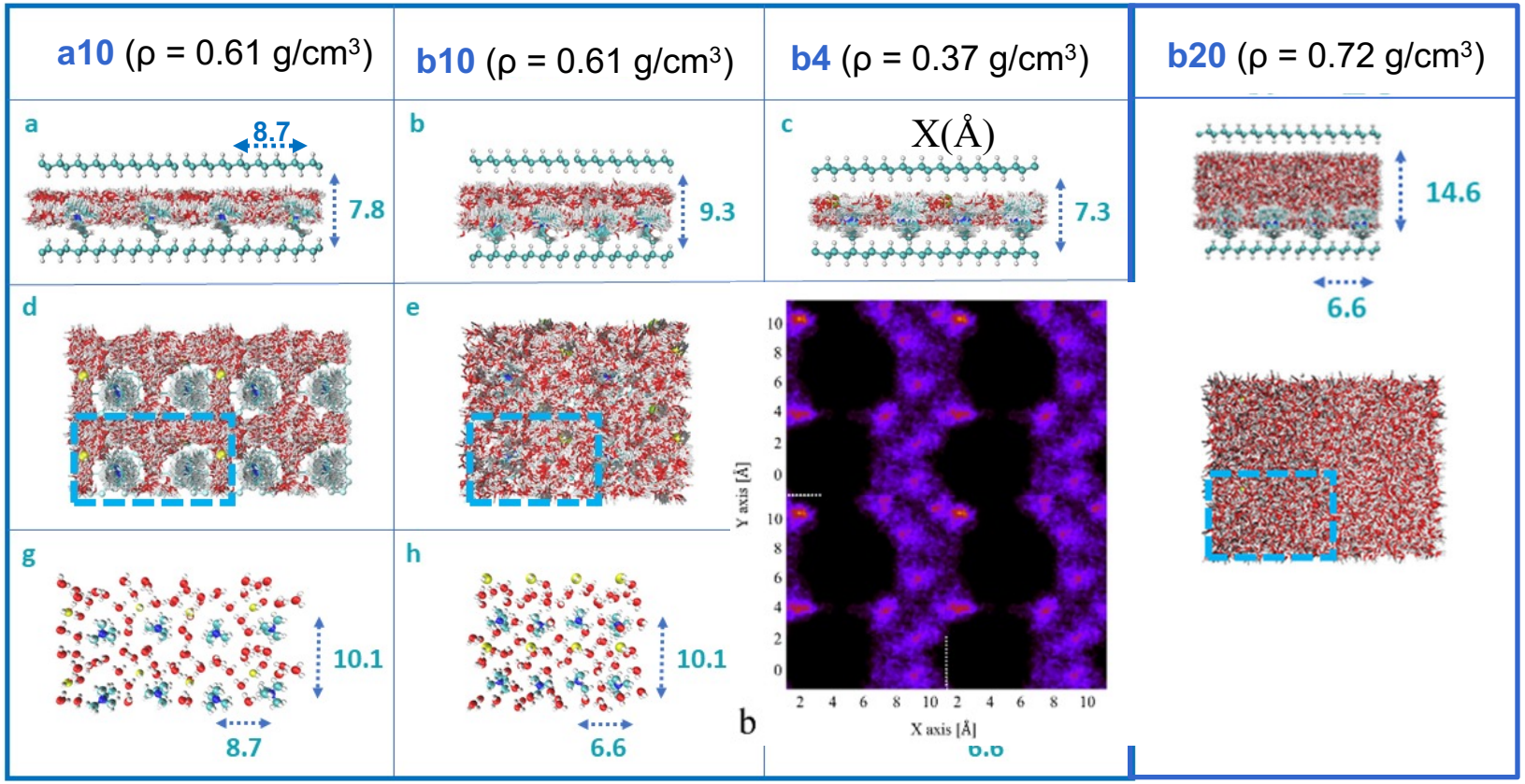

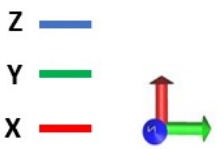

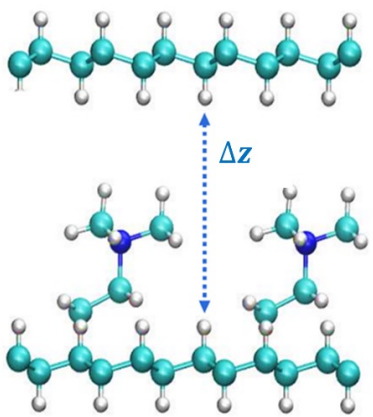

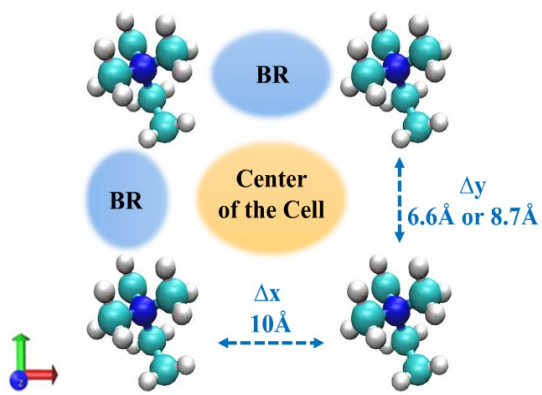

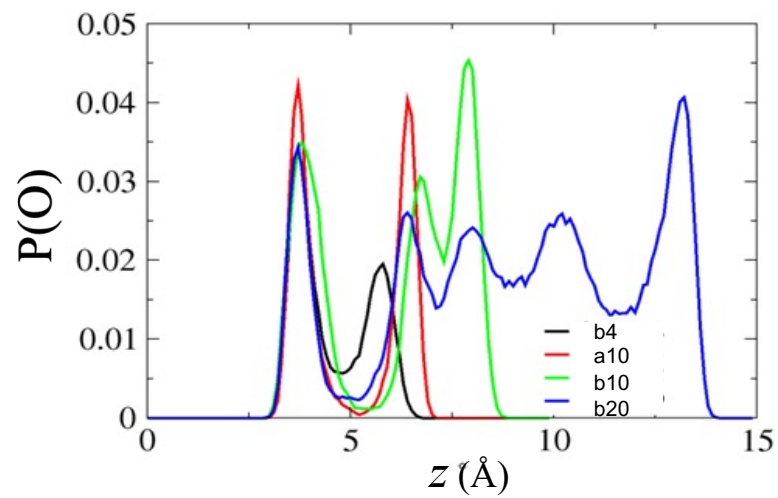

Hydroxide diffusion constants at different temperatures

$$D_{\mathrm{OH}^-} = \lim_{t\to\infty} \frac{\mathrm{d}}{\mathrm{d}t}\left|\mathbf{r}_{\mathrm{O}*}(t) - \mathbf{r}_{\mathrm{O}*}(0)\right|^2 \quad \text{including identity changes}$$

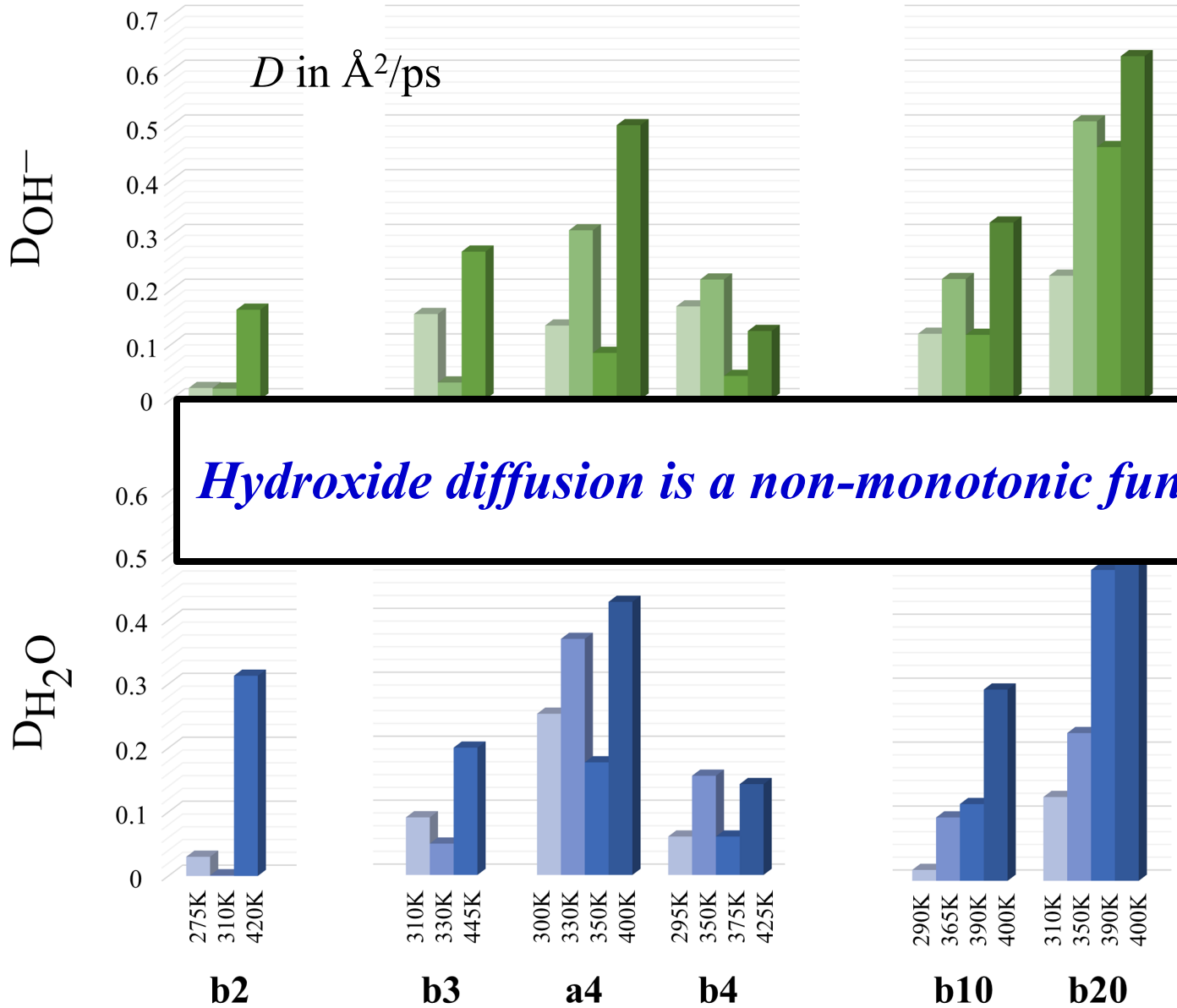

Diffusion "kink":

$$\frac{\mathrm{d}D_{\mathrm{OH}^-}}{\mathrm{d}T} < 0$$

T. Zelovich, *et al.*
***Chem. Mater.* (2022)**

Hydroxide diffusion is a non-monotonic function of T!

a10:

$$D_{\mathrm{OH}^-}^{300\mathrm{K}} = 0.076$$

$$D_{\mathrm{H_2O}}^{300\mathrm{K}} = 0.027$$

^{1}H-NMR Pulsed Field Gradient Measurements

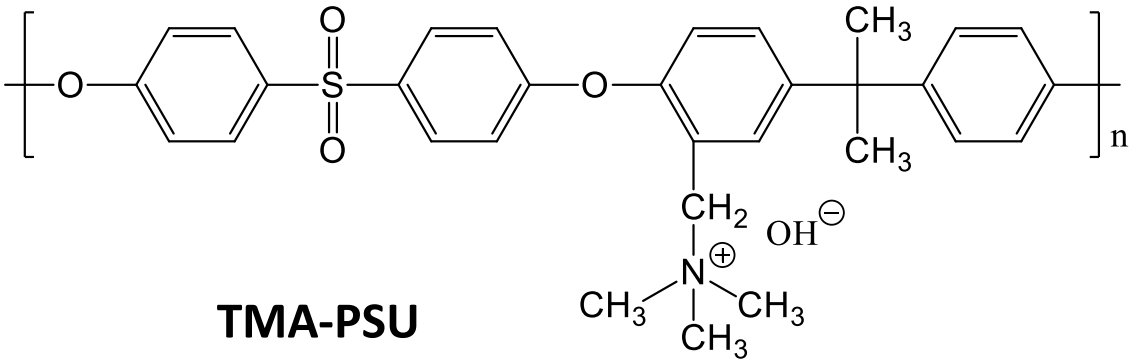

TMA-PSU
(polysulfone)

Temperature increased by 10 K every 15 mins.

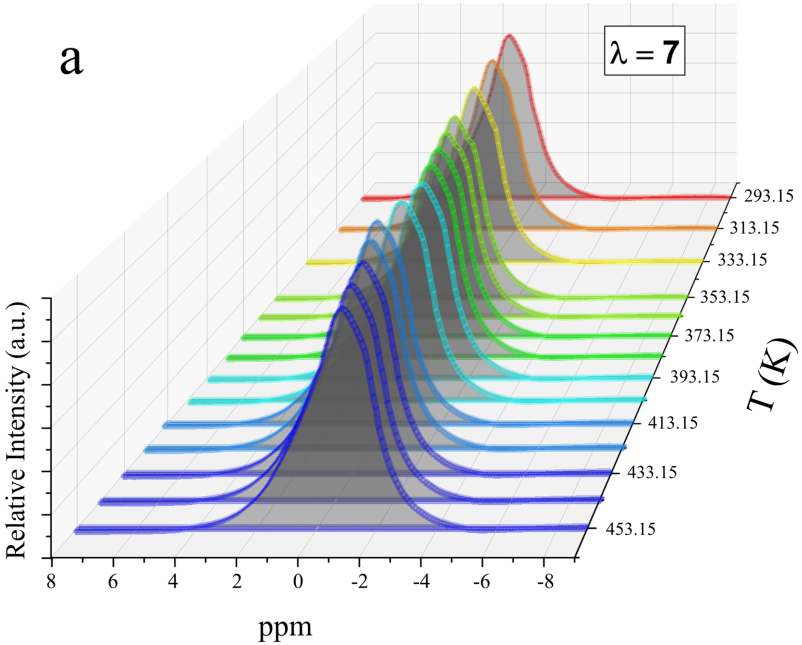

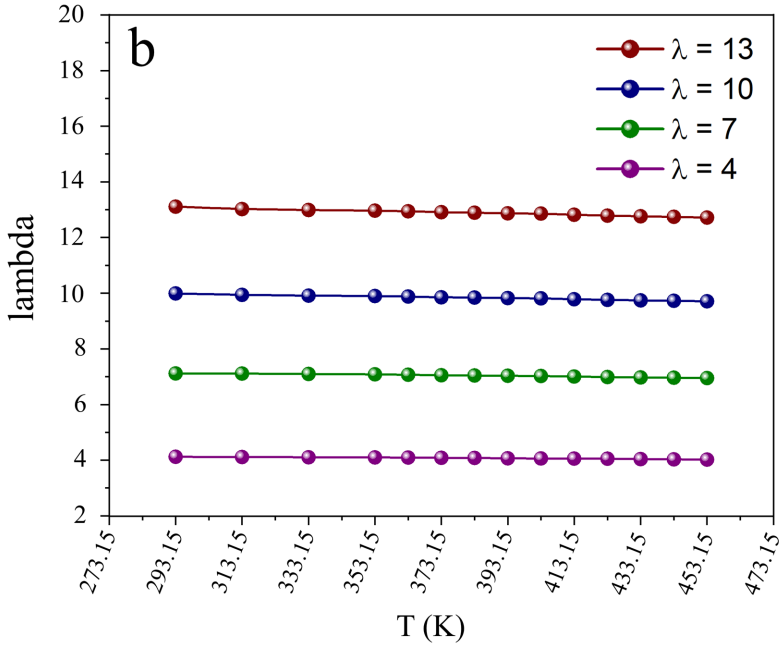

^{1}H-NMR Pulsed Field Gradient Measurements

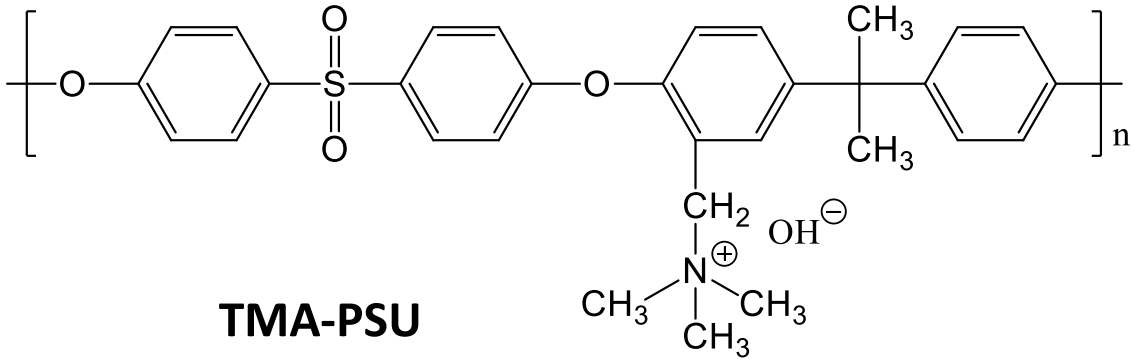

TMA-PSU

(polysulfone)

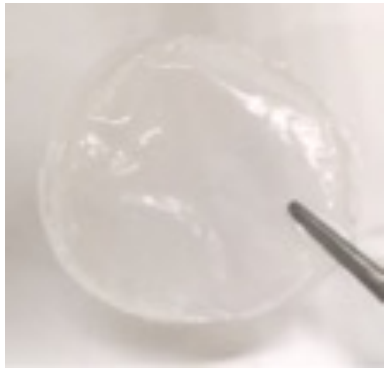

Diffusion kink region: $\frac{dD_{OH^-}}{dT} < 0$

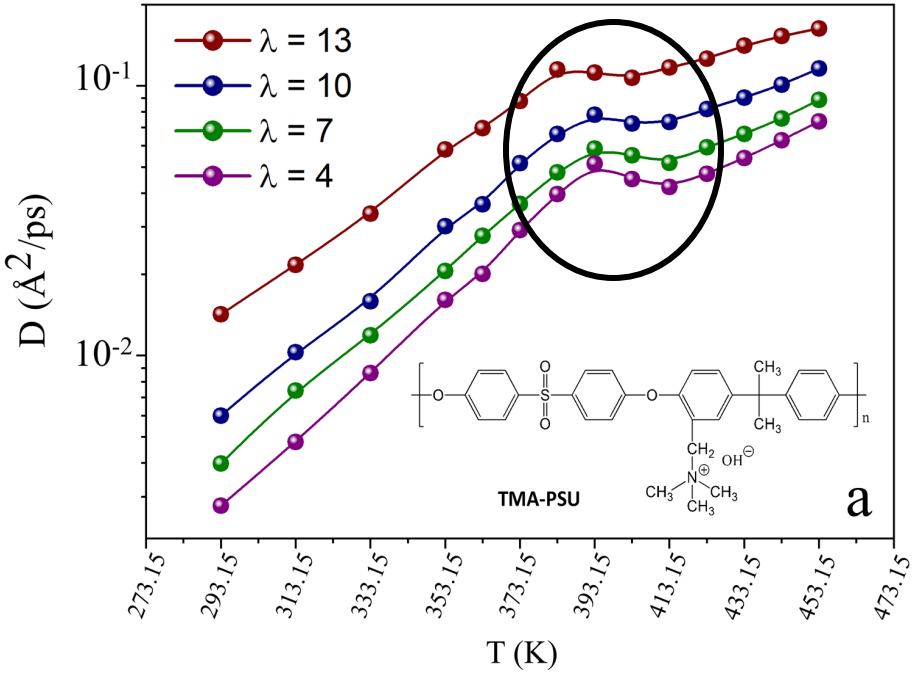

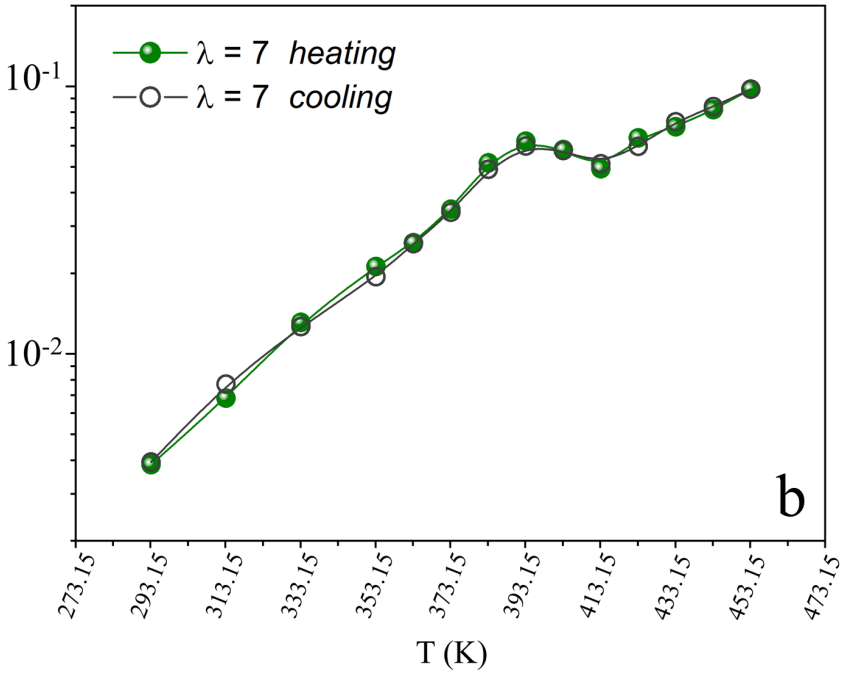

Role of water layers

b20 system:

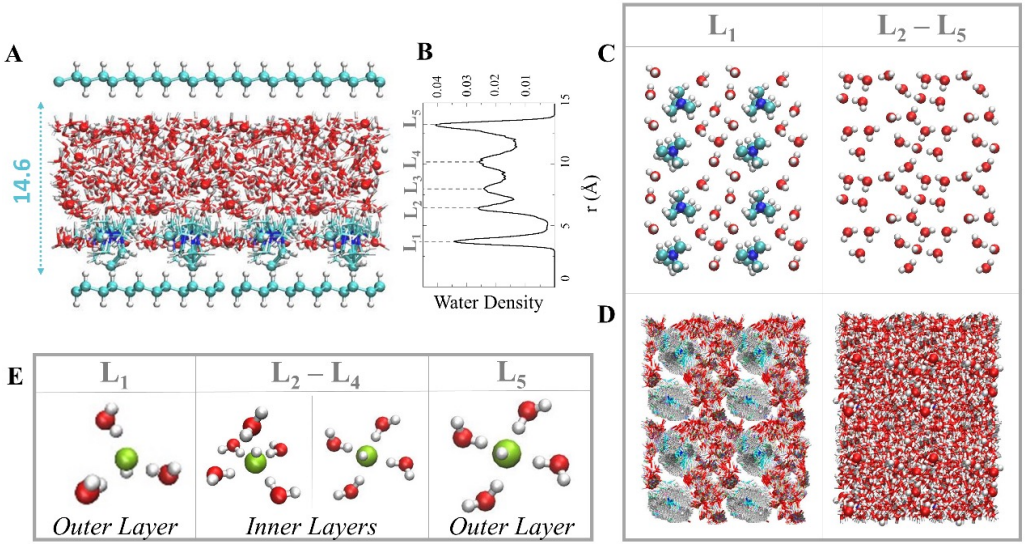

A. The Relative Time (in %) the Two Hydroxide Ions Spend in Each Water Layer

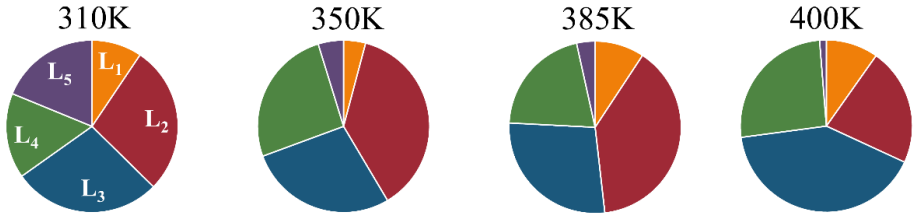

B. The Total Number of PT Events Per Water Layer

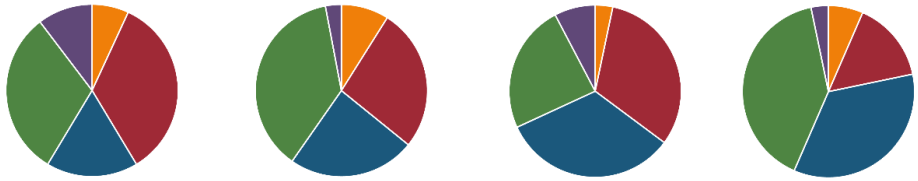

T. Zelovich and MET *J. Phys. Chem. Lett.* **11**, 5087 (2020).

Water Layer	3A+0D	3A+1D	4A+0D	4A+1D	Others
		---			---
Population probabilities	8.0	7.4	39.3	28.7	16.6
L_1	**54**	18.9	**27**	0	
L_2	7.5	10.9	**44.5**	**31.6**	
L_3-L_4	8.3	8.6	**29.8**	**36.4**	
L_5	27.8	4.9	**52.5**	11.4	
Bulk	5.1	10.4	50.5	29.9	

Z. Ma and MET *Chem. Phys. Lett.* **511**, 177 (2011)

Role of water layers in b10 system

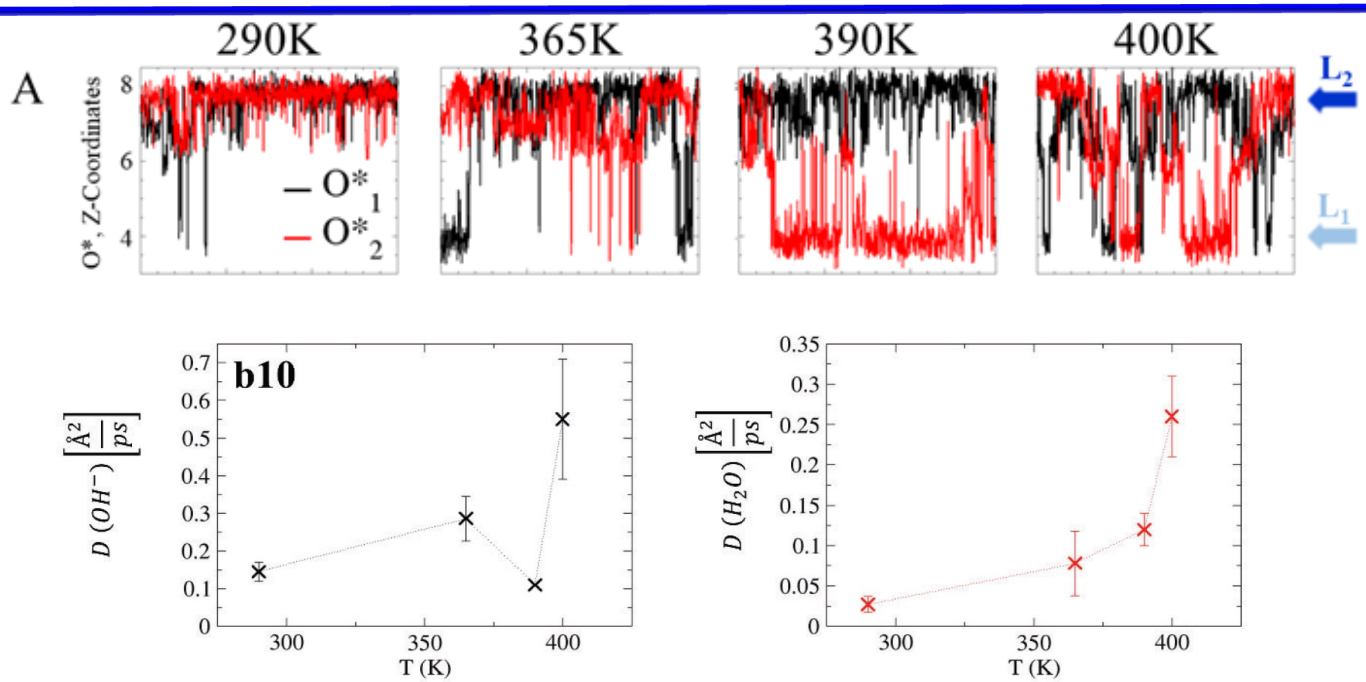

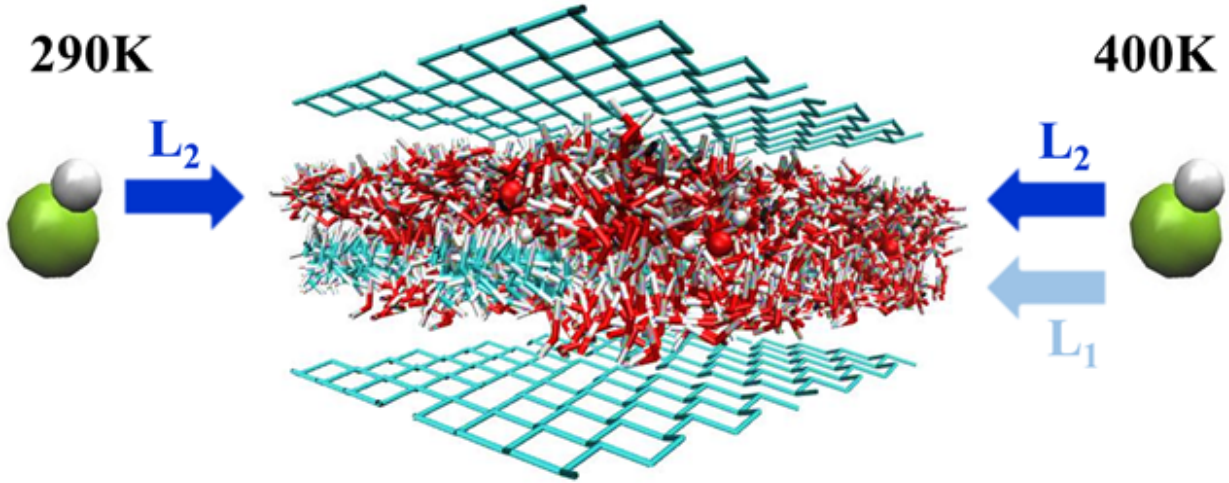

Changing cation chemistry

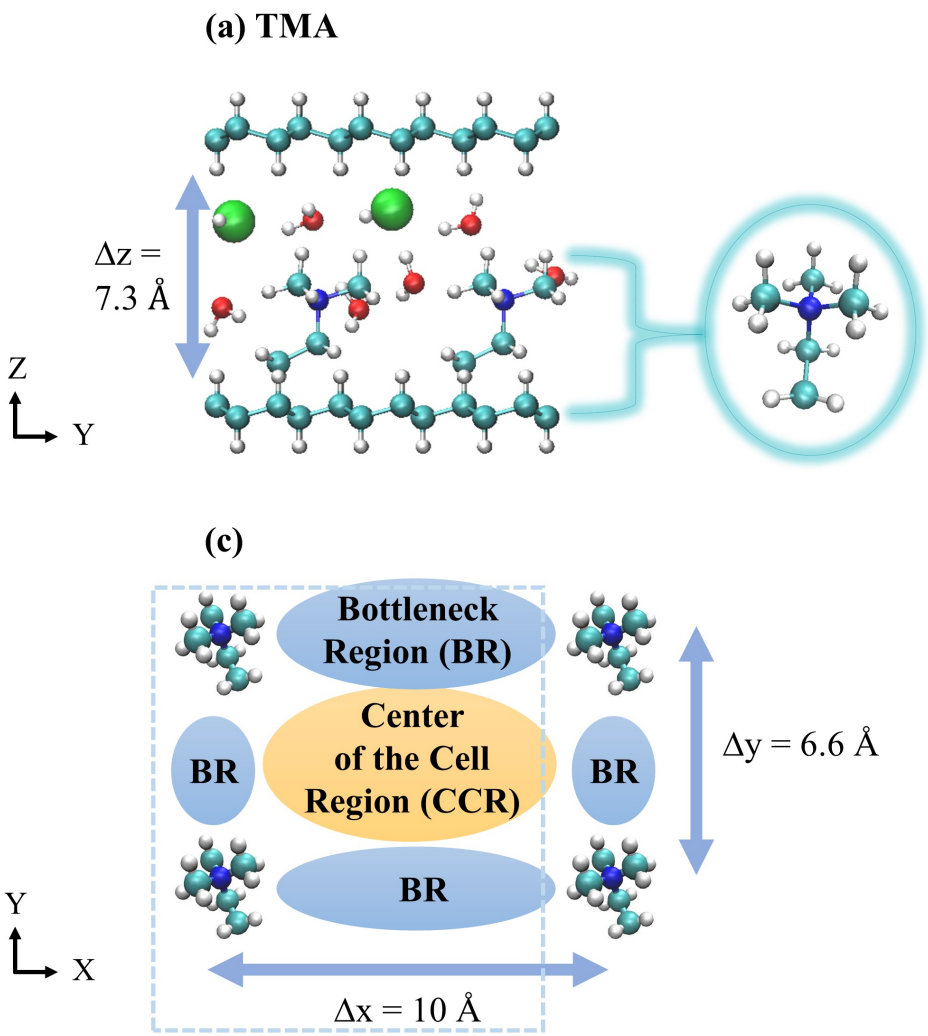

T. Zelovich, *et al. J. Membrane Sci.* (submitted)

Changing cation chemistry in b4 systems

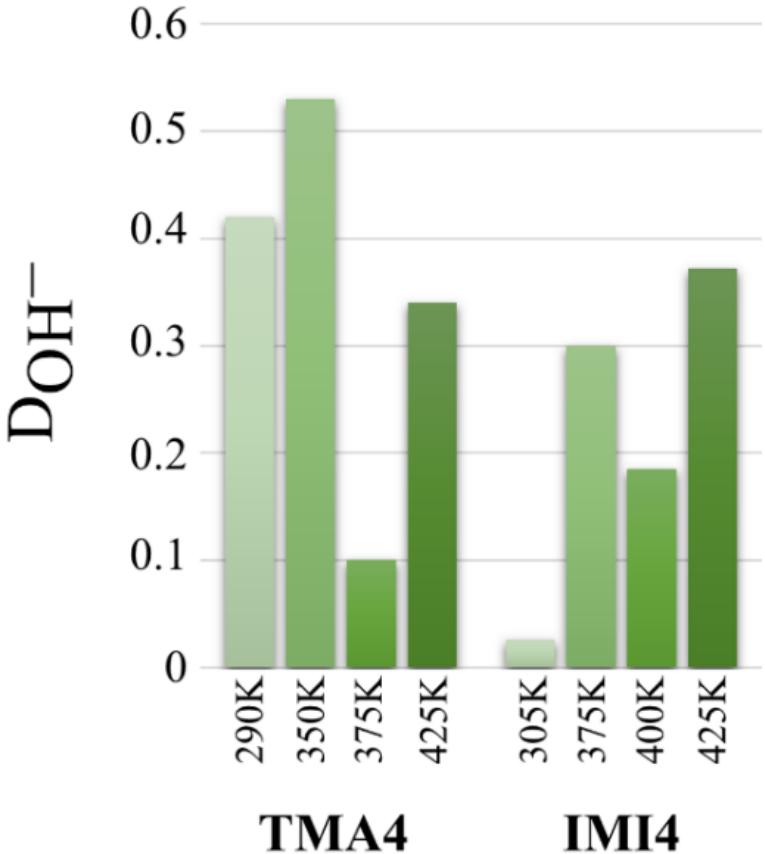

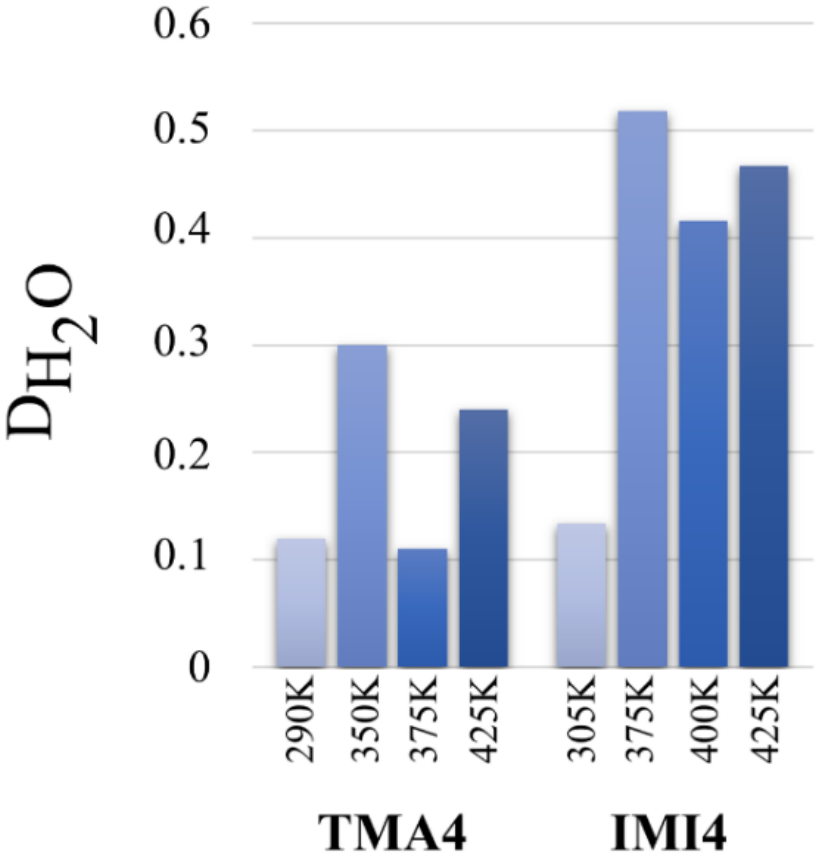

All in $Å^2/ps$

Changing cation chemistry: Water distributions

TMI, $\lambda = 4, 375$ K

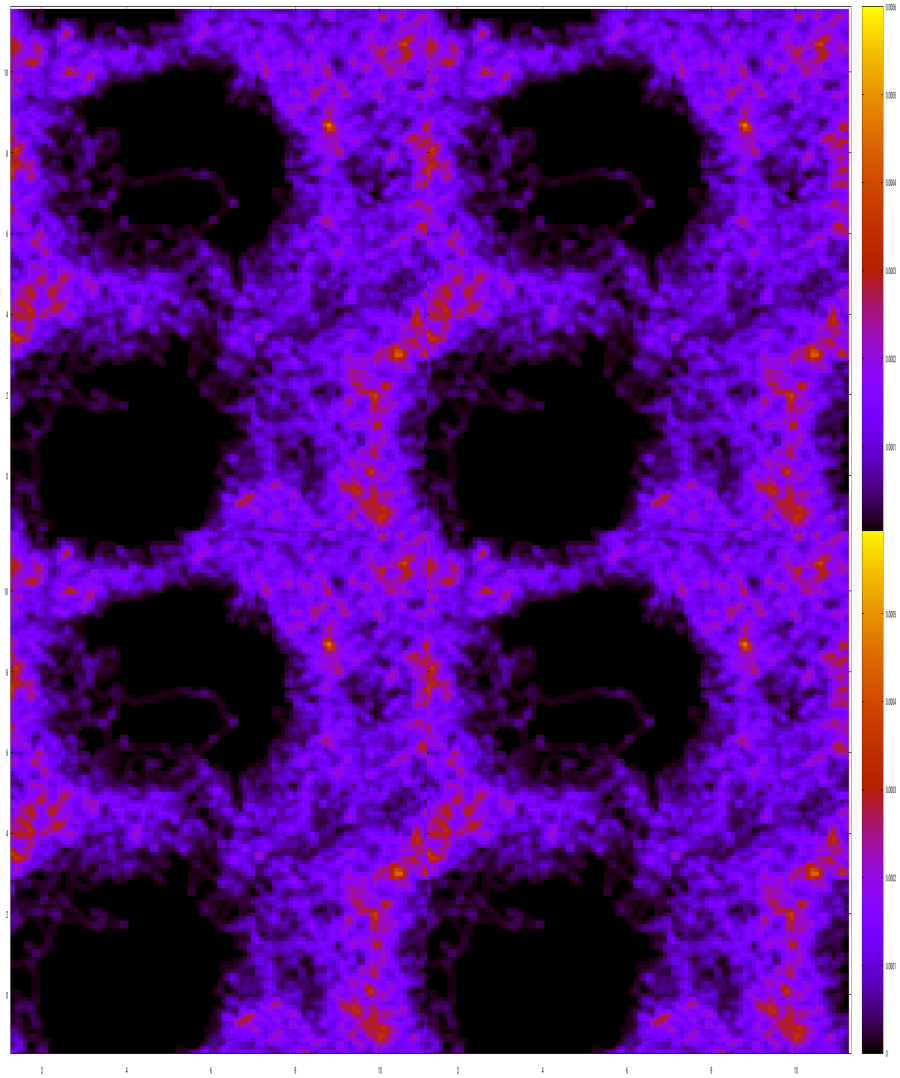

TMA, $\lambda = 4, 375$ K

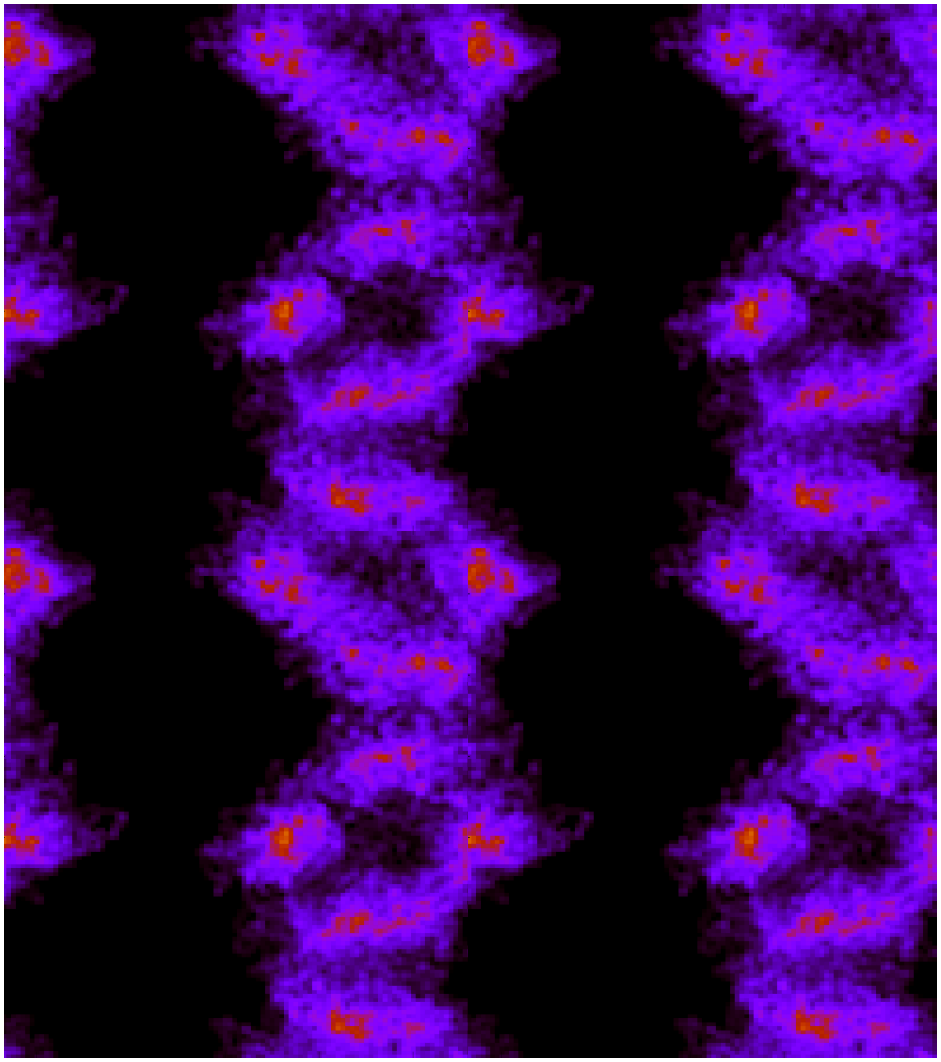

Increased diffusion and more uniform water distribution help keep the cathode hydrated, which boosts AEM fuel cell performance.

Ionic Conductivity of various Materials

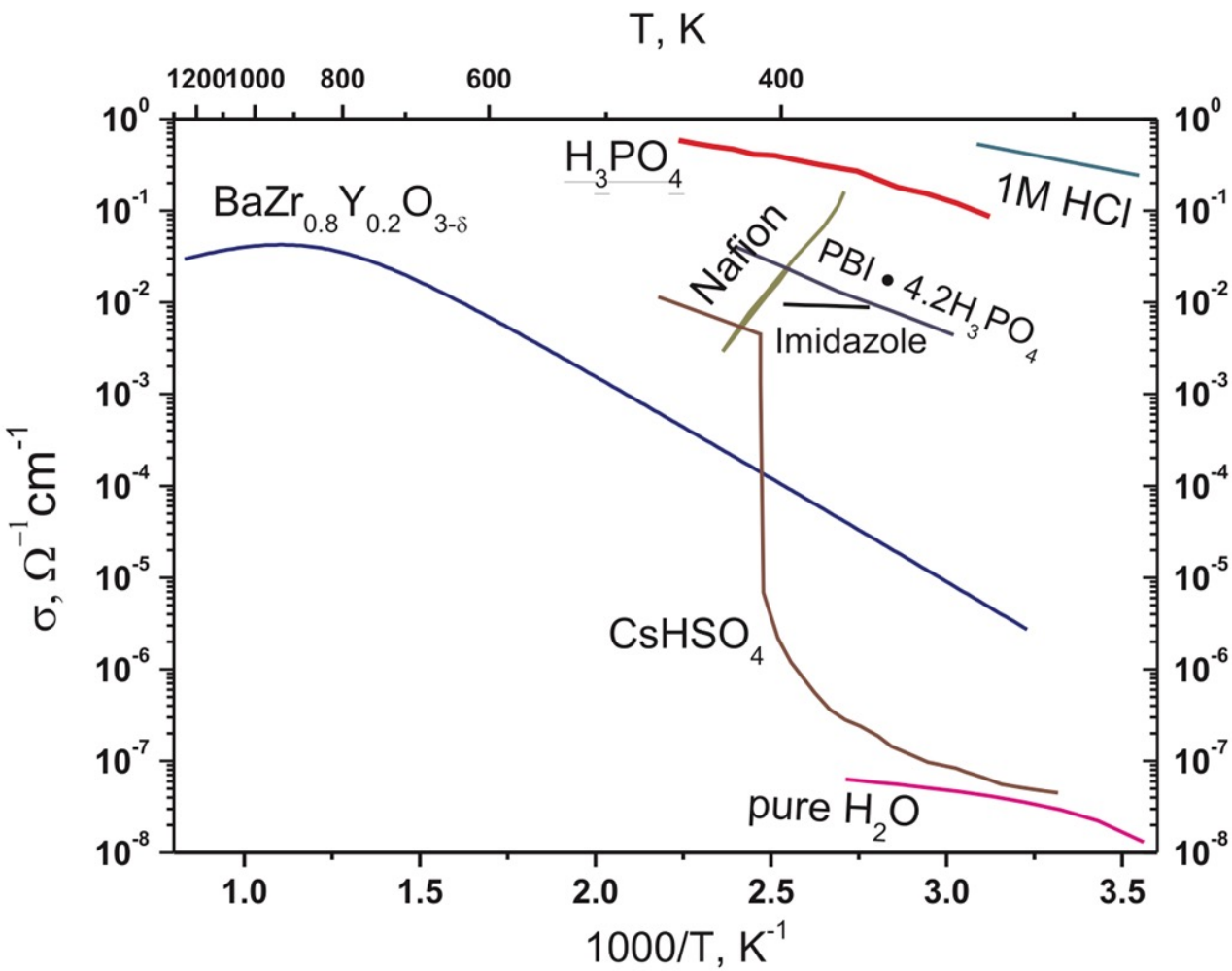

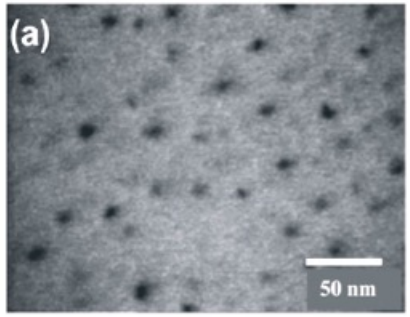

Cosby et al. PRL (2018)

High proton conductivity seen in nanoconfined liquids of derivatized Imi.

S. J. Paddison and H. A. Gasteiger, **Encyclopedia of Sustainability Science & Technology** , Springer, NY (2012).

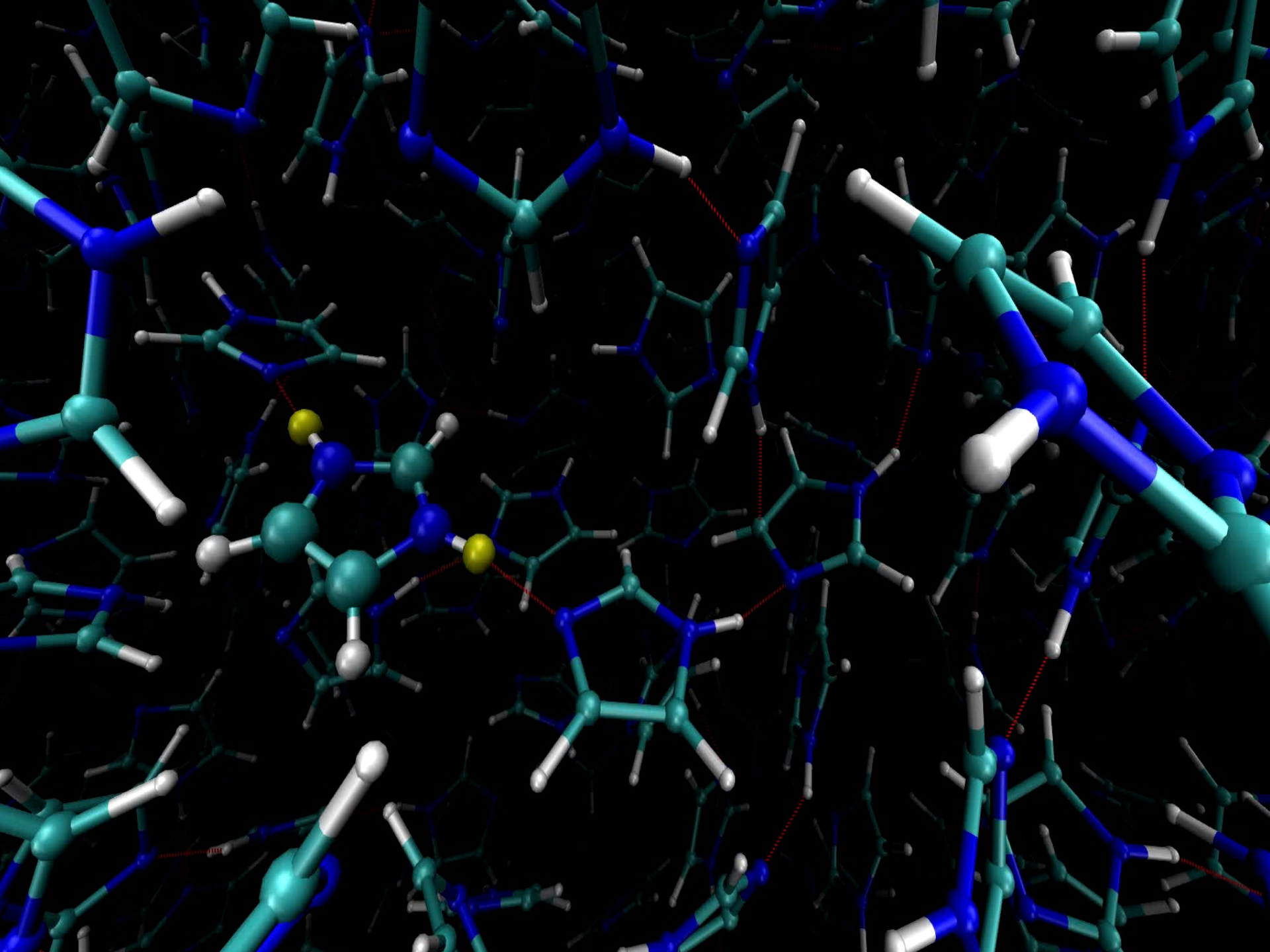

Proton transport in imidazole at 384 K

A. Chandra, MET, D. Marx *Phys. Rev. Lett.* **99,** 145901 (2007).

$$h(t) = \begin{cases} 1 & \text{if tagged molecule is Imi* at time } t. \\ 0 & \text{otherwise} \end{cases}$$

$$C_{\mathrm{i}}(t) = \frac{\langle h(0)h(t)\rangle}{\langle h\rangle}$$

$$= \sum_{k=1}^{3} a_k e^{-t/\tau_k}$$

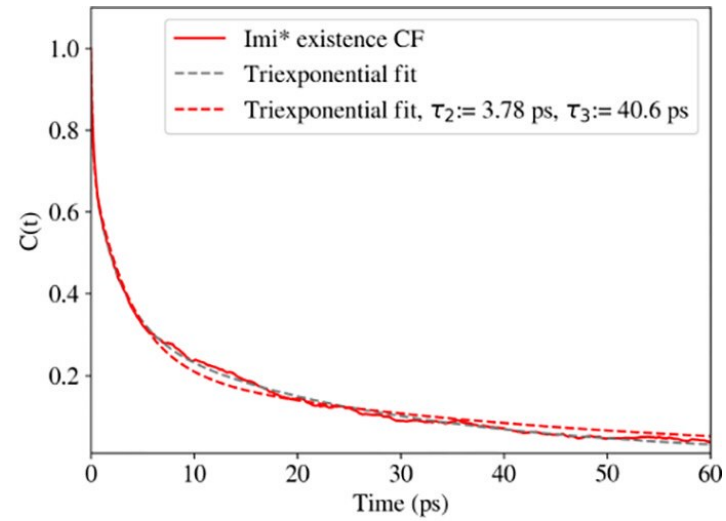

$$\langle n\rangle = 6.6$$

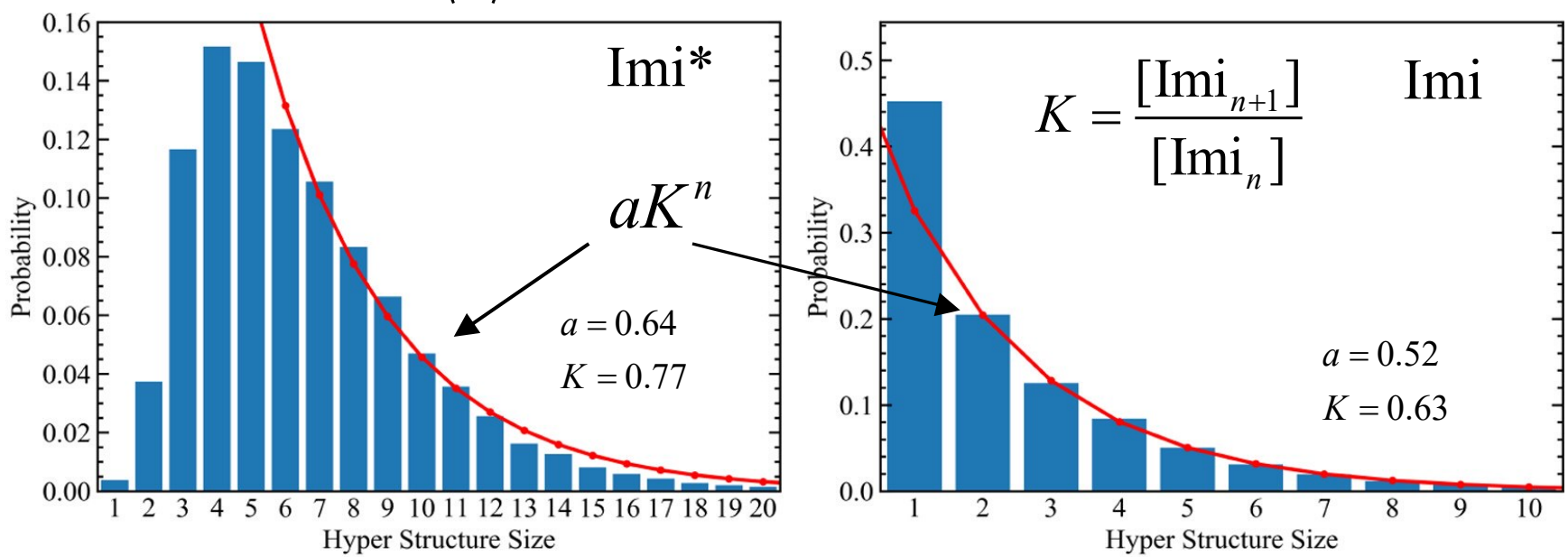

Z. R. Long, A. O. Atsango, T. E. Markland, *MET J. Phys. Chem. Lett.* **11**, 6156 (2020)

Proton transport in imidazole at 384 K

$$D_p = 0.47\ \text{Å}^2/\text{ps}$$
$$D_{\text{Imi}} = 0.06\ \text{Å}^2/\text{ps}$$

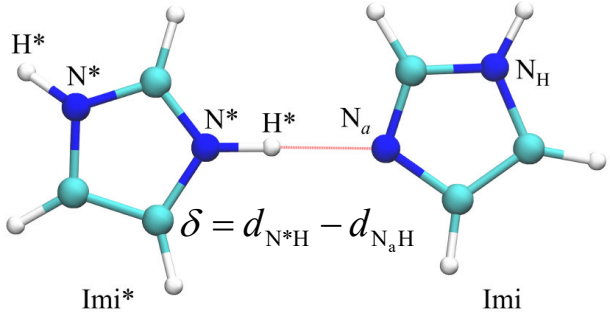

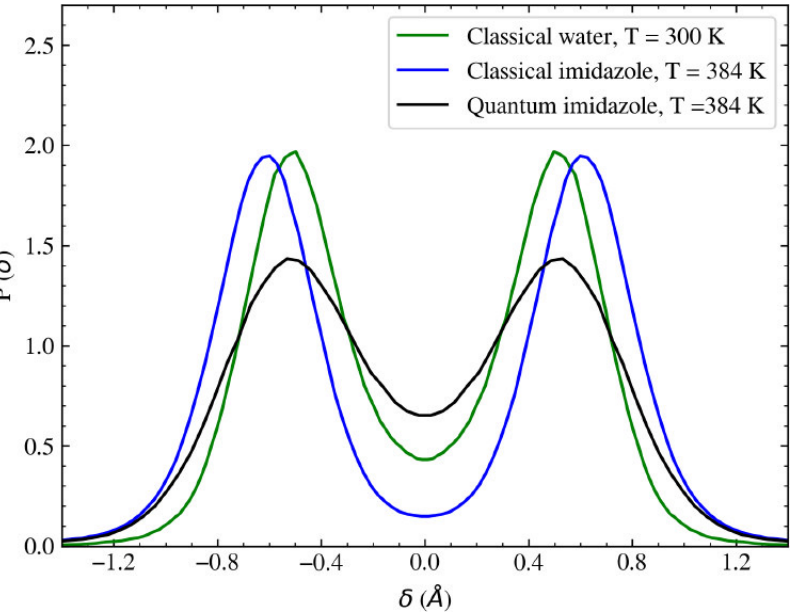

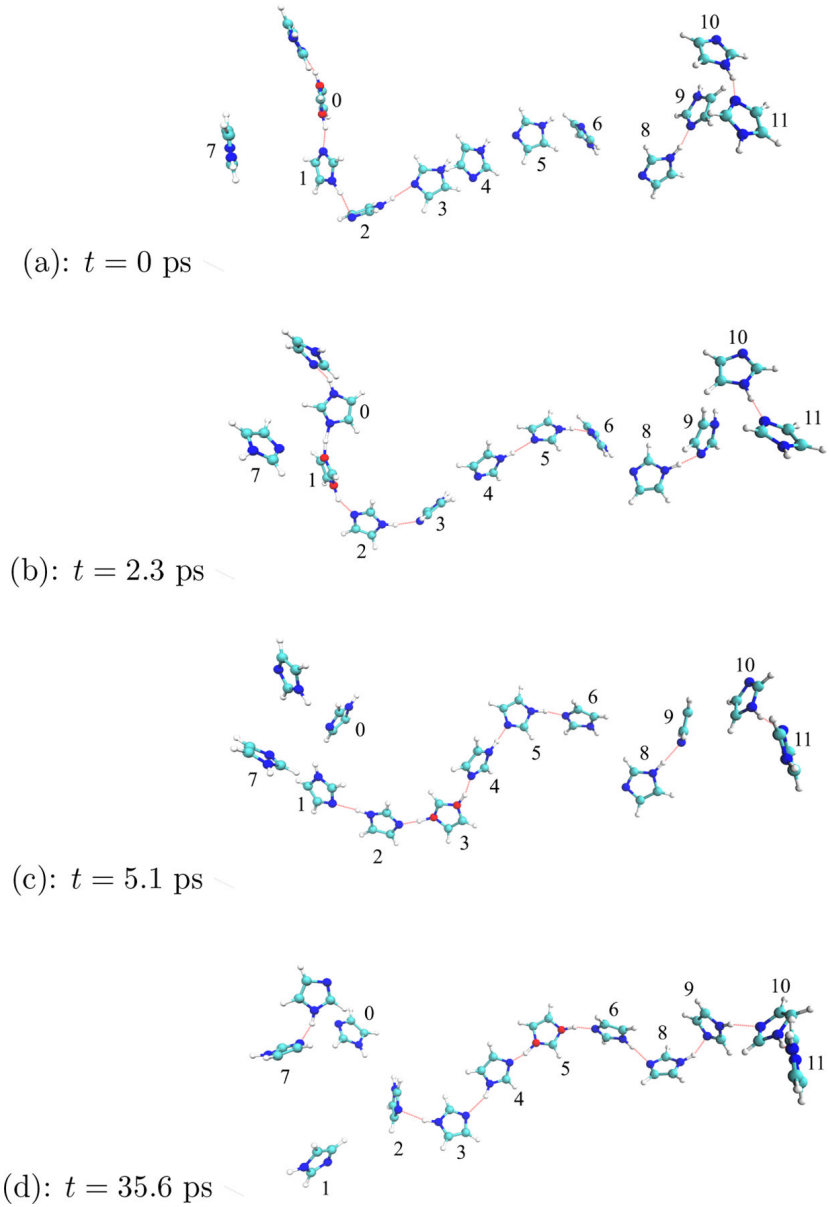

Z. R. Long, A. O. Atsango, T. E. Markland, *MET J. Phys. Chem. Lett.* **11**, 6156 (2020)

Hydrogen in structure-II clathrate

A. Witt, *et al. JPCC* (2010); J. R. Cendagorta, *et al. PCCP* (2016); J. R. Cendagorata *et al*. *Adv. Theor. Simulat*. (2021)

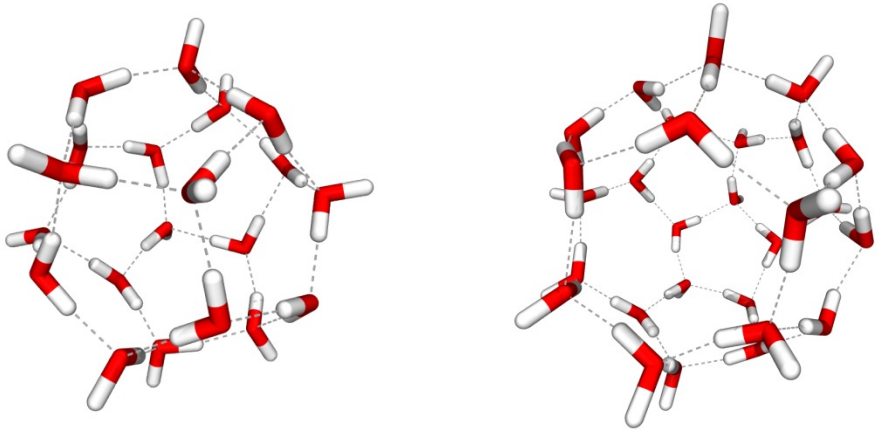

5^{12} cage $5^{12}6^{4}$ cage

Unit cell: 16 : 8

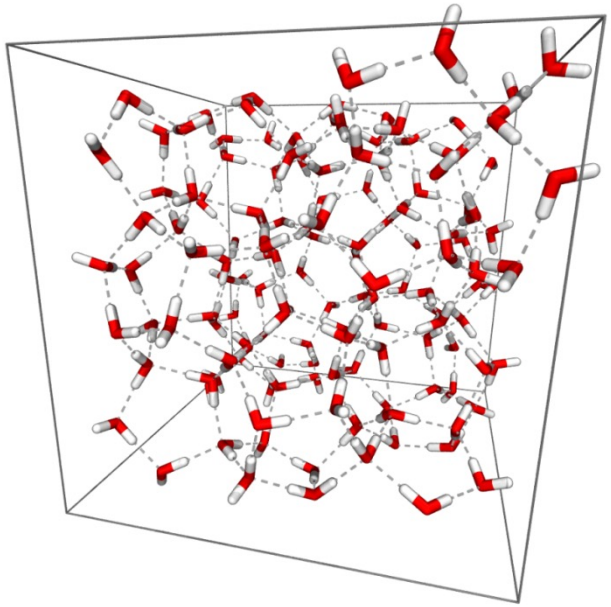

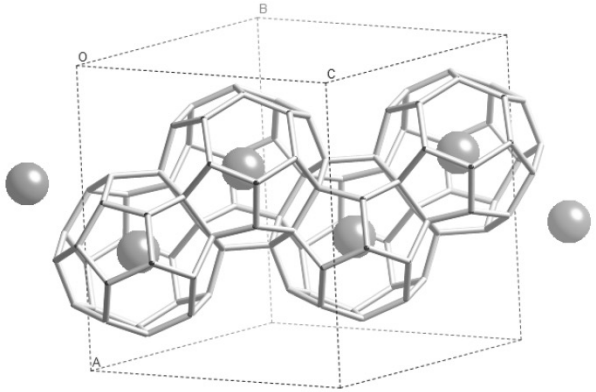

Strobel et al. (2007)

Site-site hopping model:

$$D(T) \approx \alpha k(T) l^2$$

S. Chandrasekhar (1943)

Occupancy: 4 H_2 in large cages, 1 in small cages ~ 3.8 mass %, 2 in small cages ~ 5.3 mass %
DOE target value ~ 5.5 mass %

Equilibrium nuclear quantum effects via Feynman path integrals

Quantum equilibrium properties derived from the canonical partition function:

$$Z(\beta) = \mathrm{Tr}\left[e^{-\beta\hat{H}}\right] = \int d\mathbf{r}\ \left\langle \mathbf{r}\middle| e^{-\beta(\hat{T}+\hat{V})} \middle|\mathbf{r}\right\rangle$$

$$= \lim_{P\to\infty} \int d\mathbf{r}_1 \cdots d\mathbf{r}_P \prod_{i=1}^{P} \left\langle \mathbf{r}_i \middle| \hat{\Omega} \middle| \mathbf{r}_{i+1} \right\rangle_{\mathbf{r}_{P+1}=\mathbf{r}_1}, \qquad \hat{\Omega} = e^{-\beta\hat{T}/P} e^{-\beta\hat{V}/P}$$

$$Z_P(\beta) \equiv \left(\frac{mP}{2\pi\beta\hbar^2}\right)^{3P/2} \int d\mathbf{r}_1 \cdots d\mathbf{r}_P \exp\left\{-\sum_{i=1}^{P}\left[\frac{mP}{2\beta\hbar^2}\left(\mathbf{r}_i - \mathbf{r}_{i+1}\right)^2 + \frac{\beta}{P}V(\mathbf{r}_i)\right]\right\}\Bigg|_{\mathbf{r}_{P+1}=\mathbf{r}_1}$$

Classical particle

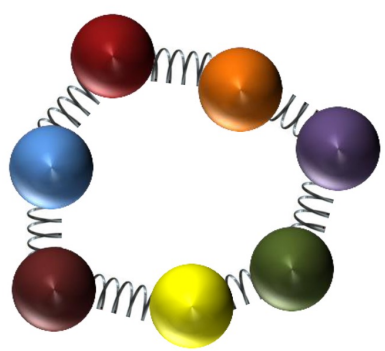

Quantum particle (thermodynamic view)

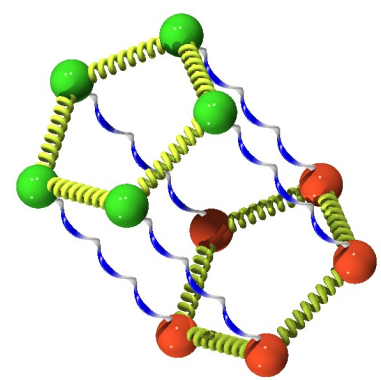

Interacting quantum particles

Creating a neural network potential [Behler and Parrinello *PRL* (2007)]

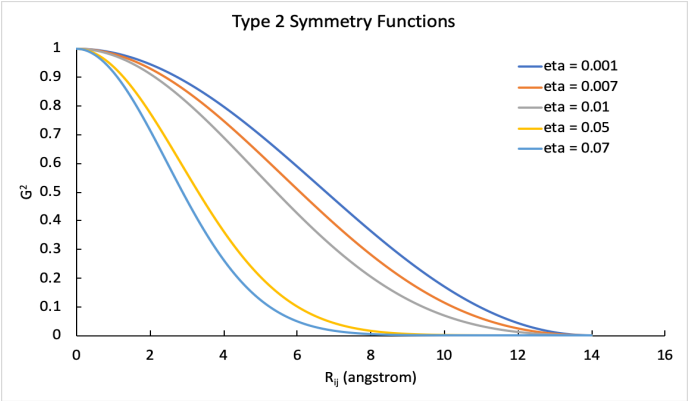

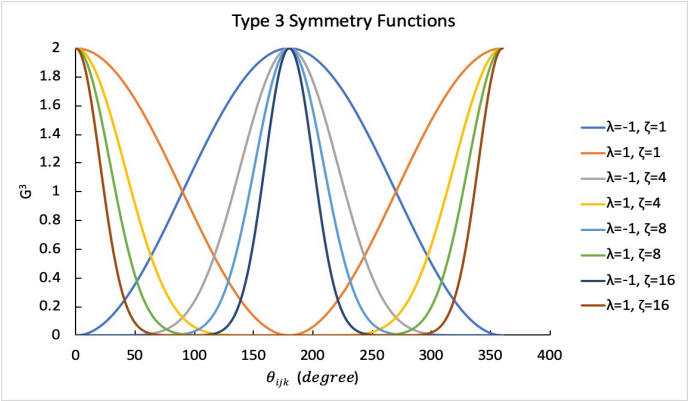

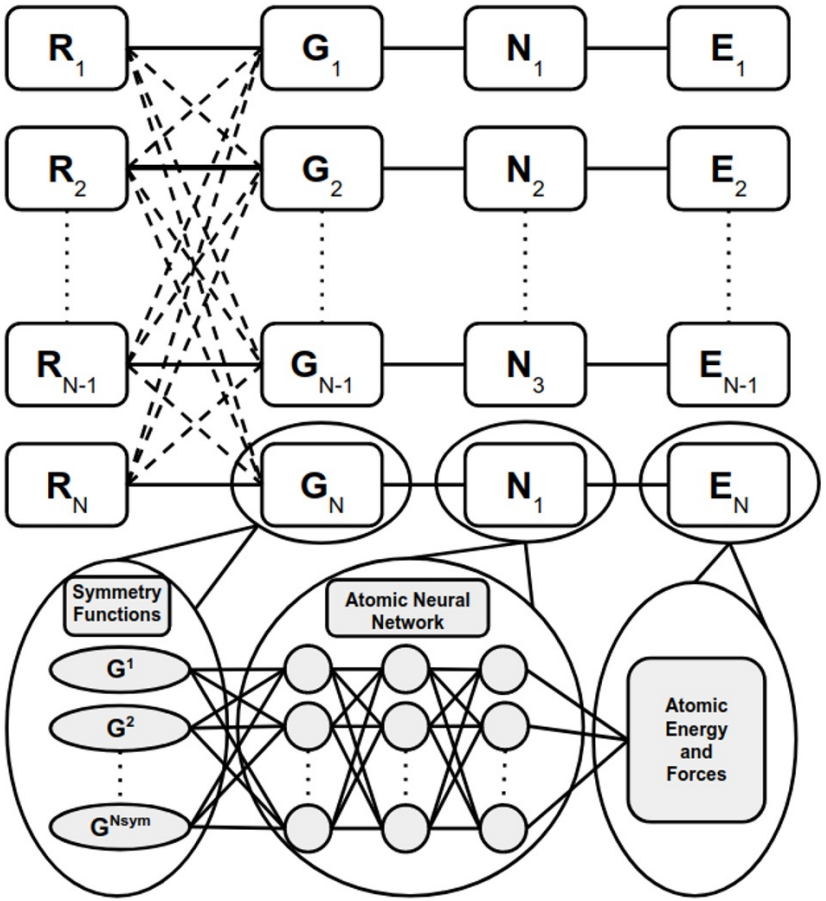

$$G_i^2 = \sum_{j=1}^{N_{\text{atom}}} e^{-\eta\left(R_{ij}-R_s\right)^2} f_c(R_{ij})$$

3 Networks: O_w, H_w, H_2

Trained to revPBE0 + D3 dispersion

$$G_i^3 = 2^{1-\zeta} \sum_{j\neq k} \sum_{k\neq i,j} \left[\left(1+\lambda\cos\theta_{ijk}\right)^{\zeta} e^{-\eta\left(R_{ij}^2+R_{ik}^2+R_{jk}^2\right)} f_c(R_{ij}) f_c(R_{ik}) f_c(R_{jk}) \right]$$

Creating a neural network potential [Behler and Parrinello *PRL* (2007)]

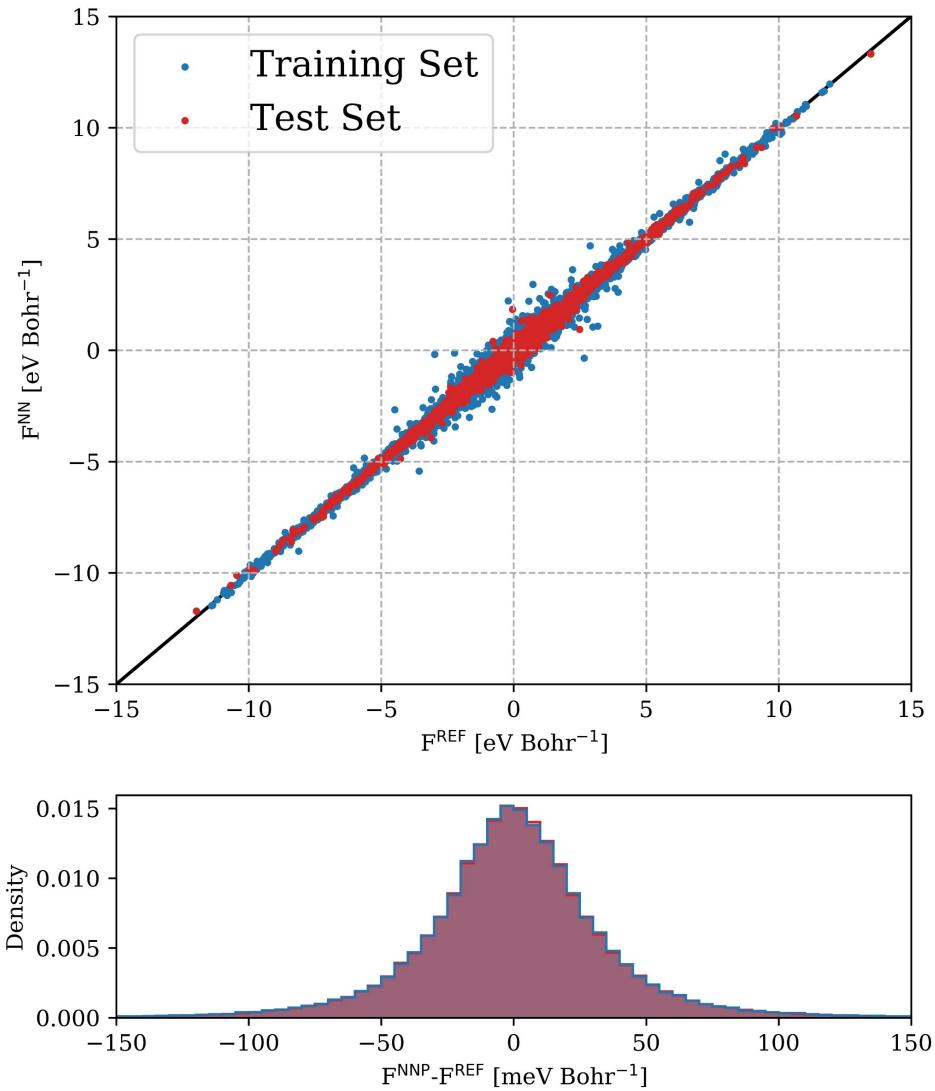

Training data:

- 1,600 configurations of a water box with 64 molecules
- 3,000 configurations of a H_2 box with 56 molecules
- 500 configurations of an H_2 + H_2O box of different compositions.
- 500 actual H_2+clathrate configurations.

Unit cell of Mak *et al.*
JCP (1965)

Quantum
Classical

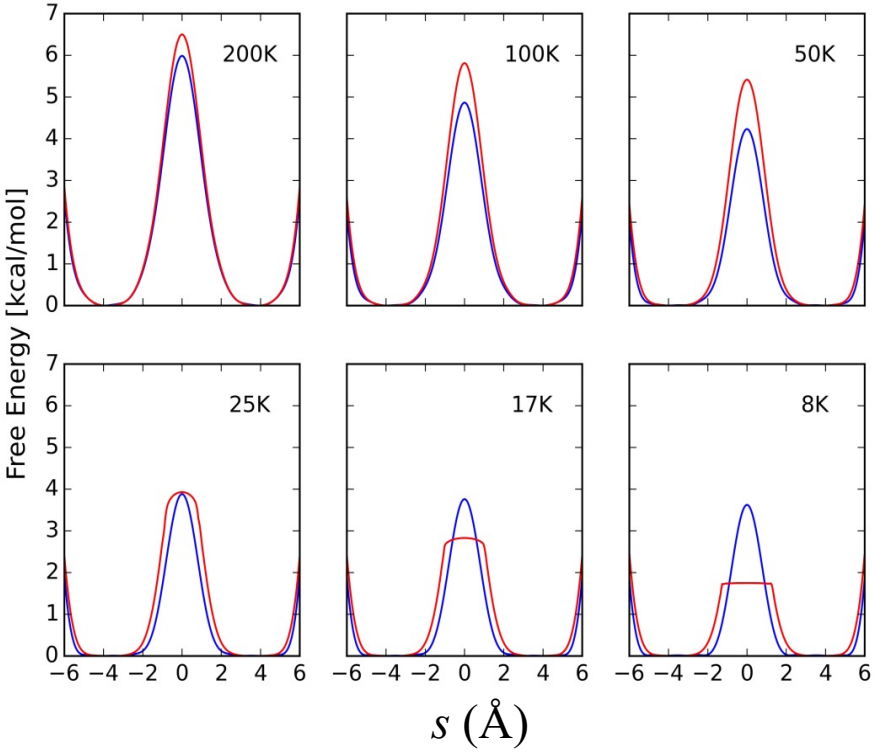

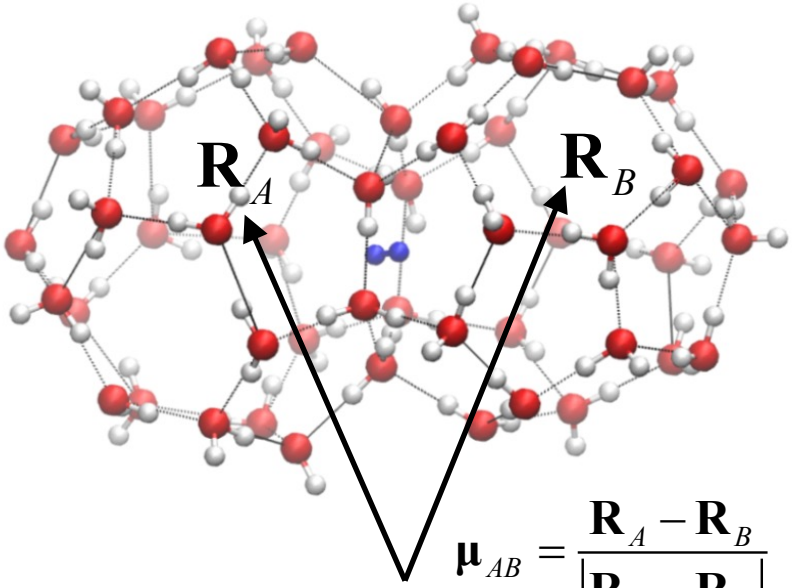

$$\boldsymbol{\mu}_{AB} = \frac{\mathbf{R}_A - \mathbf{R}_B}{\left|\mathbf{R}_A - \mathbf{R}_B\right|}$$

$$q(\mathbf{r}) = \left[\frac{1}{2}\left(\mathbf{r}_{\mathrm{H}_1} + \mathbf{r}_{\mathrm{H}_2}\right) - \mathbf{R}_A\right] \bullet \boldsymbol{\mu}_{AB} - \frac{\left|\mathbf{R}_B - \mathbf{R}_A\right|}{2}$$

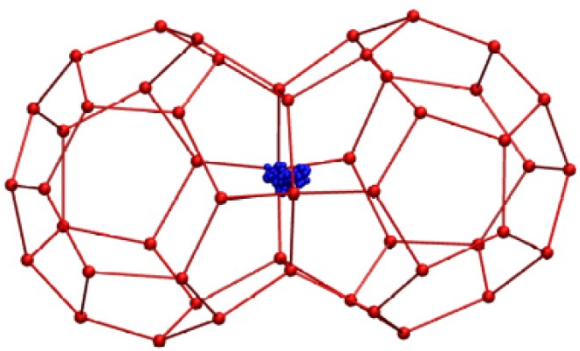

50 K

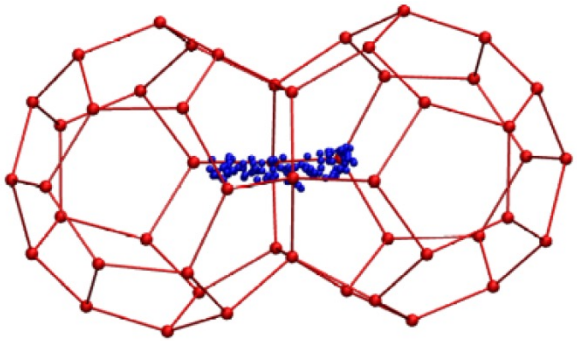

25 K

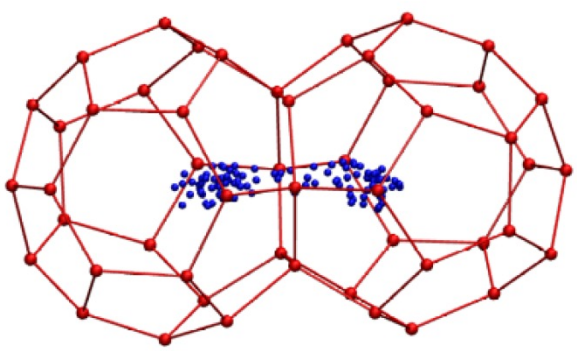

8 K

Quantum rates from ring-polymer molecular dynamics

R. Craig and D. E. Manolopoulos *J. Chem. Phys*. (2005)
T. J. H. Hele and S. C. Althorpe *J. Chem. Phys*. (2013)

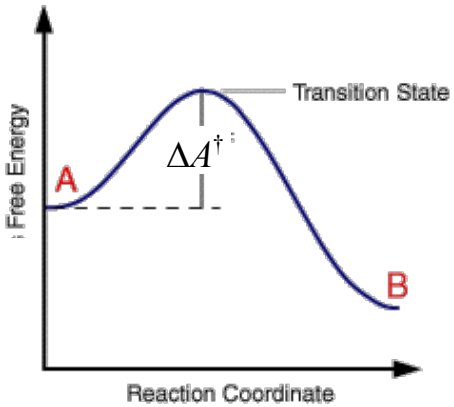

Quantum rate coefficient:

$$k(\beta) = \frac{1}{Z_r(\beta)} \lim_{t\to\infty} C_{\mathrm{fs}}(t)$$

Flux-side correlation function:

$$C_{\mathrm{fs}}(t) = \mathrm{Tr}\left[\hat{F}(q^\dagger) e^{i\tau^* \hat{H}/\hbar} \theta(\hat{q}(\hat{\mathbf{r}}) - q^\dagger I) e^{-i\tau \hat{H}/\hbar}\right], \qquad \tau = t - \frac{i\beta\hbar}{2}$$

Flux operator

$$\hat{F}(q^\dagger) = \frac{1}{2m}\left[\hat{p}\delta\left(\hat{q}(\hat{\mathbf{r}}) - q^\dagger I\right) + \delta\left(\hat{q}(\hat{\mathbf{r}}) - q^\dagger I\right)\hat{p}\right]$$

RPMD approximation:

$$k(\beta) \approx k_{\mathrm{RPMD}}(\beta) = \frac{p(q_c^\dagger)}{\sqrt{2\pi\beta\mu}} \lim_{t\to\infty} \kappa(t)$$

Quantum rates from ring-polymer molecular dynamics

Reaction-coordinate probability

$$p(q_c^\dagger) = \frac{e^{-\beta\Delta F(q_c^\dagger)}}{\int_{q_r}^{q^\dagger} dq_c \; e^{-\beta\Delta F(q_c)}}$$

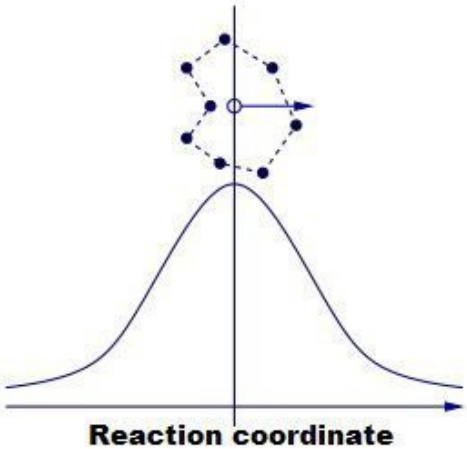

$\kappa(t)$ is computed from ring-polymer molecular dynamics

[I. R. Craig and D. E. Manolopoulos *J. Chem. Phys*. **121**, 3368 (2004)]

$$H_P = \sum_{i=1}^{P} \frac{\mathbf{p}_i^2}{2m} + \frac{1}{2} m P \omega_P^2 \sum_{i=1}^{P} (\mathbf{r}_{i+1} - \mathbf{r}_i)^2 + \sum_{i=1}^{P} V(\mathbf{r}_i), \qquad \omega_P = \frac{\sqrt{P}}{\beta\hbar}$$

Equations of motion:

$$\dot{\mathbf{r}}_i = \frac{\mathbf{p}_i}{m}, \qquad \dot{\mathbf{p}}_i = -mP\omega_P^2 \left(2\mathbf{r}_i - \mathbf{r}_{i+1} - \mathbf{r}_{i-1}\right) - \frac{\partial V}{\partial \mathbf{r}_i}$$

Unit cell of Mak *et al.*
JCP (1965)

Quantum
Classical

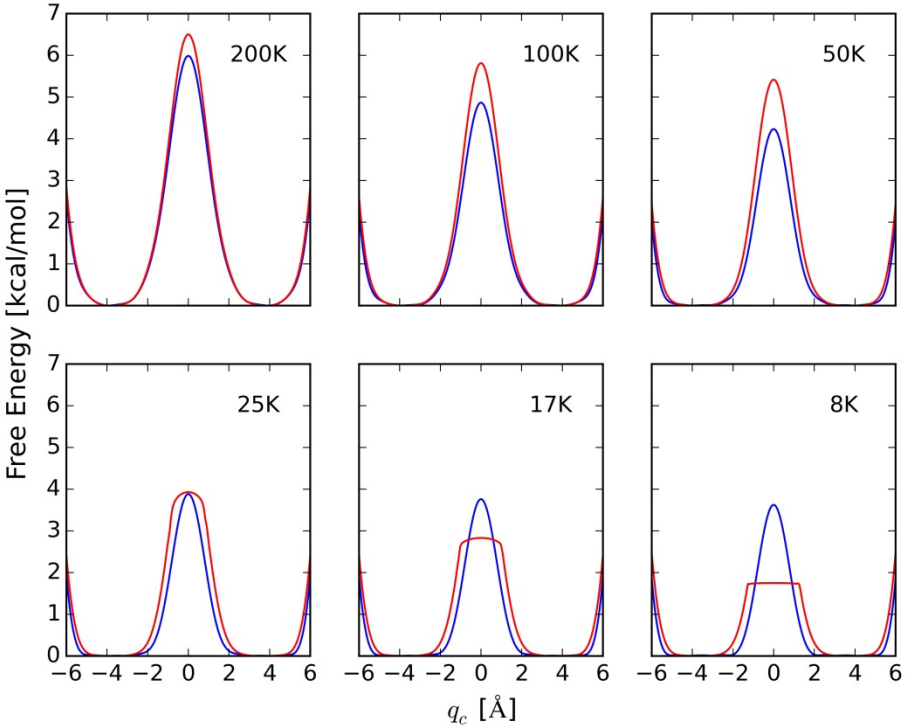

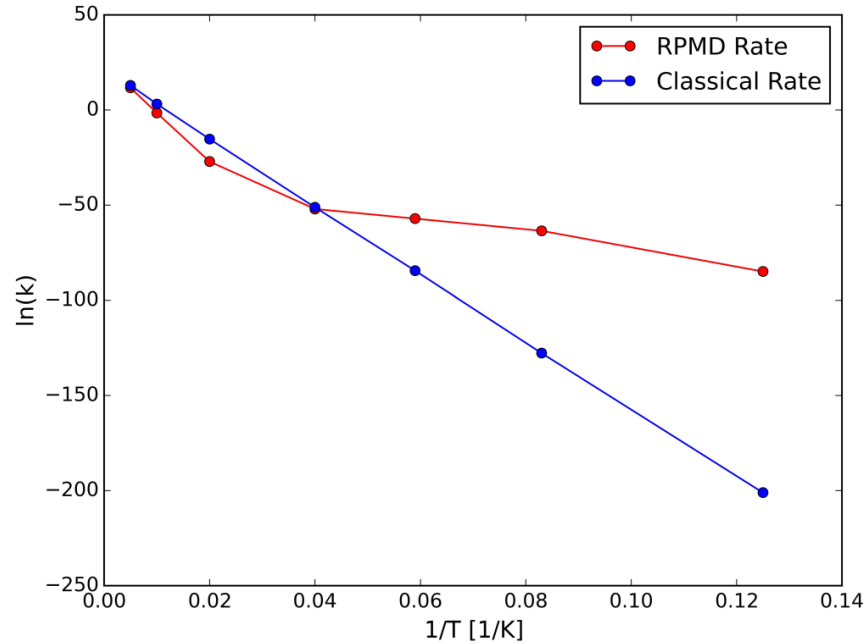

$$q(\mathbf{r}) = \left[\frac{1}{2}\left(\mathbf{r}_{\mathrm{H}_1} + \mathbf{r}_{\mathrm{H}_2}\right) - \mathbf{R}_A\right] \bullet \boldsymbol{\mu}_{AB} - \frac{\left|\mathbf{R}_B - \mathbf{R}_A\right|}{2}$$

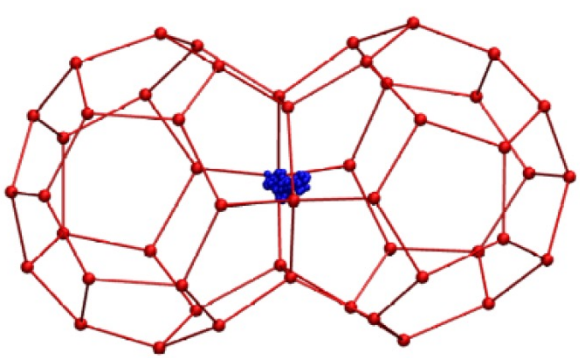

50 K

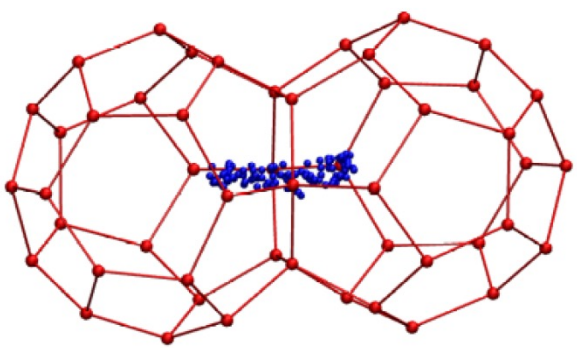

25 K

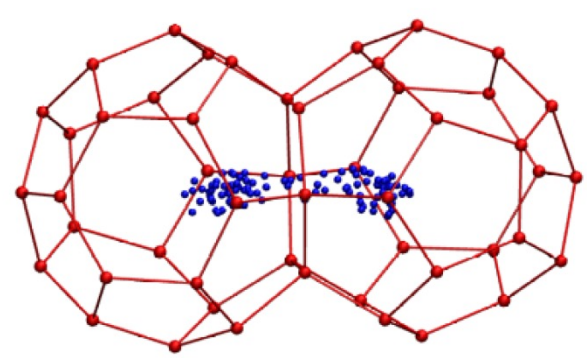

8 K

Sampling the hydrogen cage-hopping events at 25 K

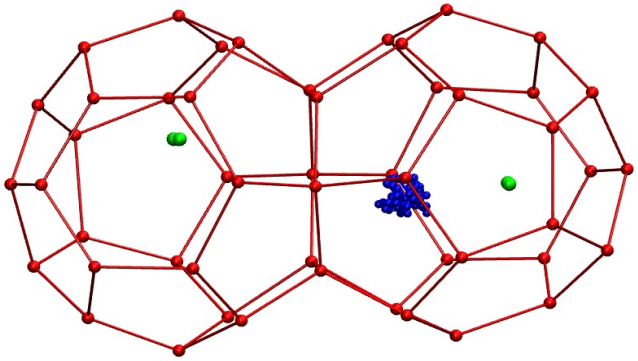

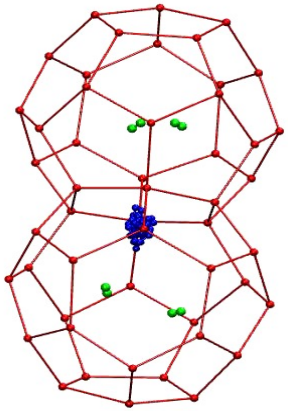

First results at 120 K

Solvation Process	Chemical Potential [kcal mol^{-1}]
$\{0\} \rightarrow \{1\}$	-5.6 ($\pm$ 0.01)
$\{1\} \rightarrow \{2\}$	-4.1 ($\pm$ 0.02)
$\{2\} \rightarrow \{3\}$	-3.9 ($\pm$ 0.02)
$\{3\} \rightarrow \{4\}$	-4.2 ($\pm$ 0.02)

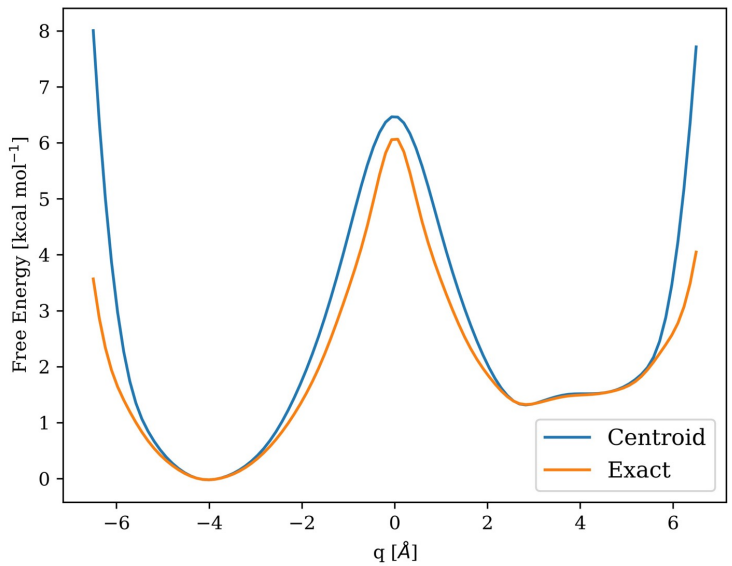

Experimental barrier estimate from NMR: 3.8 kcal/mol.
[Senadheera, Conradi *JPCB* (2007)]

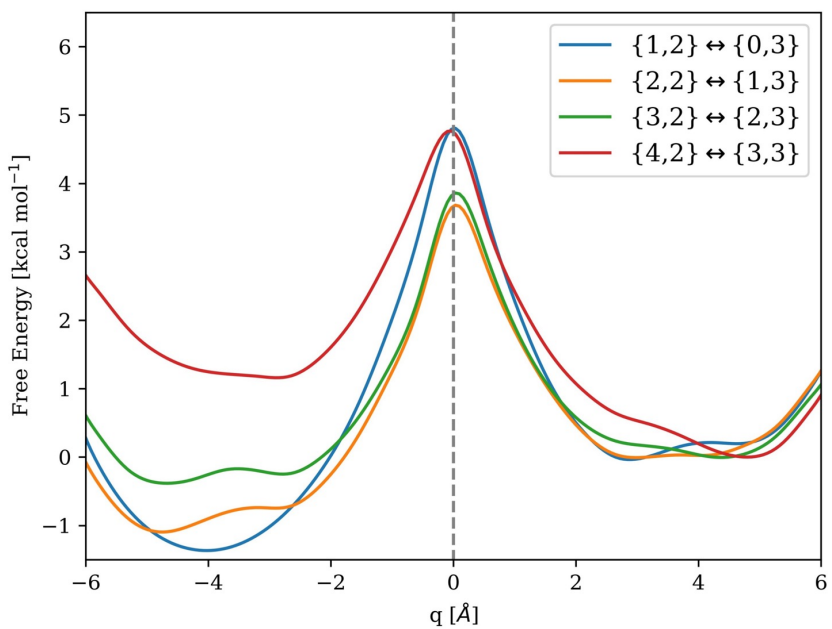

Acknowledgements

Stephen J. Paddison
Chemical/Biomolecular Engineering
University of Tennessee

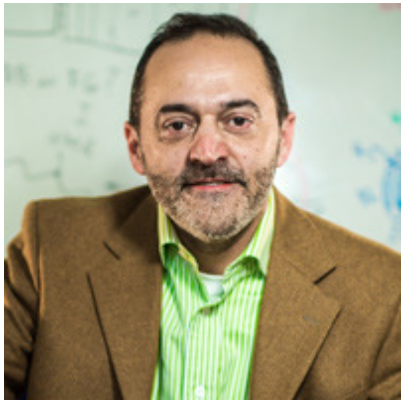

Dario Dekel
Chemical Engineering
Technion

Dr. Tamar Zelovich
NYU

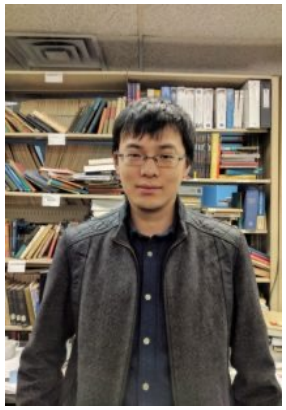

Zhuoran Long
Yale University

Isabella Nicotera
Department of Physics
Universita della Calabria

Joseph Cendagorta
Data Scientist
Ashland Chemicals

Ondrej Marsalek
Institute of Physics
Charles University, CR

Tom Markland
Dept. of Chemistry
Stanford University